Article

What triggers explosive radiations and mass extinctions? A unified critical transition framework

WenJun Zhang
School of Life Sciences, Sun Yat-sen University, Guangzhou, China
E-mail: zhwj@mail.sysu.edu.cn, wjzhang@iaees.org

Received 3 April 2026; Accepted 21 April 2026; Published online 30 May 2026; *Published 1 September 2026*

Abstract
The two most dramatic phenomena in the history of life, explosive evolutionary radiations and catastrophic mass extinctions, have traditionally been studied as separate problems with distinct causal mechanisms. This paper challenges that divide by proposing that both are manifestations of a single underlying process: the crossing of critical thresholds in a complex adaptive system. I conceptualize the global ecosystem as a high-dimensional ecological landscape whose topography is jointly shaped by three macroscopic order parameters, system resilience *R*, environmental pressure *S*, and evolutionary potential *I*. Through a unified mathematical framework combining stochastic differential equations, network percolation theory, and the physics of critical transitions, I show that mass extinctions correspond to collapse transitions occurring when environmental stress overwhelms a system whose resilience has been eroded, while evolutionary radiations correspond to innovation transitions occurring when accumulated evolutionary potential breaches a nucleation threshold under permissive conditions. The model predicts that both types of transition are preceded by detectable early-warning signals, critical slowing down, increasing variance, and rising autocorrelation, that arise from the same dynamical origin. Network percolation provides the mechanistic link: the fragmentation of the ecological interaction network below a critical connectivity defines the collapse cascade, whereas the re-establishment of a percolating network of novel interactions defines the radiation cascade. The theory resolves long-standing puzzles, including the synchronicity of the Cambrian explosion, the variable magnitude of mass extinctions under similar external forcings, and the frequently delayed recoveries following extinction events. Applied to the contemporary biodiversity crisis, the framework yields a sobering quantitative prediction: the simultaneous erosion of functional redundancy and modularity (decreasing *R*) coupled with accelerating climatic and chemical perturbations (increasing *S*) is driving the modern biosphere toward a collapse threshold, and early-warning indicators are already detectable in multiple ecological time series. The unified criticality model thus offers both a retrospective understanding of life's grandest ebbs and flows and a prospective tool for anticipating the next potential mass extinction.

Keywords macroevolutionary dynamics; critical transitions; mass extinction; evolutionary radiation; ecological resilience; network percolation; early-warning signals; complex adaptive systems.

Proceedings of the International Academy of Ecology and Environmental Sciences
ISSN 2220-8860
URL: http://www.iaees.org/publications/journals/piaees/online-version.asp
RSS: http://www.iaees.org/publications/journals/piaees/rss.xml
E-mail: piaees@iaees.org
Editor-in-Chief: WenJun Zhang
Publisher: International Academy of Ecology and Environmental Sciences

1 The Two Extremes in the History of Life

1.1 Problem Statement

The history of life on Earth is punctuated by two contrasting yet equally dramatic macroevolutionary phenomena: the sudden proliferation of biodiversity known as evolutionary radiations, and the catastrophic collapse of biodiversity known as mass extinctions. The Cambrian explosion, occurring approximately 540 to 520 million years ago, witnessed the relatively rapid appearance of most animal phyla in the fossil record, establishing the fundamental body plans that have persisted throughout the Phanerozoic (Erwin and Valentine, 2013; Marshall, 2006). In stark contrast, the end-Permian mass extinction approximately 252 million years ago eliminated more than 90% of marine species and approximately 70% of terrestrial vertebrate families in a geologically brief interval (Benton, 2003; Erwin, 2006). These two phenomena represent the extreme ends of a spectrum of macroevolutionary dynamics: one characterized by explosive creativity, the other by wholesale destruction.

The central puzzle that motivates this paper is whether these two classes of phenomena are fundamentally distinct processes requiring entirely separate explanatory frameworks, or whether they are, in fact, two manifestations of a deeper, unified dynamical logic. The dominant tradition in paleobiology has been to treat evolutionary radiations and mass extinctions as separate research domains, each with its own suite of causal hypotheses and analytical methods (Raup and Sepkoski, 1982; Jablonski, 2008). This fragmentation has hindered the development of a coherent theoretical understanding of how and why biodiversity changes through deep time.

1.2 The Fragmented State of Current Research

Research on evolutionary radiations has largely focused on developmental innovations, ecological opportunity, and environmental triggers. The Cambrian explosion, the most celebrated example, has been attributed to a variety of factors including rising atmospheric and oceanic oxygen concentrations (Knoll and Carroll, 1999; Sperling et al., 2013), the evolution of key developmental genetic toolkits such as the Hox gene complex (Carroll, 2006; Erwin and Davidson, 2002), ecological escalations including the advent of predation (Marshall, 2006), and nutrient influxes associated with tectonic and climatic changes (Brasier and Lindsay, 2001). Each of these hypotheses captures an important dimension of the problem, yet none alone provides a sufficient explanation for the extraordinary synchronicity and taxonomic breadth of the event. As one review noted, the Cambrian explosion had multiple causes, and different aspects of the event are best explained by different causes (Erwin and Valentine, 2013). The question remains: what systemic property of the biosphere enabled such a rapid, multi-clade radiation?

Research on mass extinctions has developed along a parallel but largely separate track. The Cretaceous-Paleogene mass extinction, driven by the Chicxulub asteroid impact approximately 66 million years ago, represents the most firmly established case of an extraterrestrial trigger (Schulte et al., 2010; Morgan et al., 2022). The end-Permian and end-Triassic mass extinctions are strongly associated with the emplacement of large igneous provinces, the Siberian Traps and the Central Atlantic Magmatic Province respectively (Burgess et al., 2014; Davies et al., 2017; Whiteside et al., 2010). The Late Ordovician mass extinction has been linked to Gondwanan glaciation and associated sea-level fluctuations (Finnegan et al., 2011; Harper, Hammarlund and Rasmussen, 2014). The Late Devonian mass extinction has been attributed to widespread marine anoxia potentially triggered by terrestrial nutrient influx from expanding land plants (Smart et al., 2023). Across these diverse triggers, a common feature is the involvement of major perturbations to the global carbon cycle, typically expressed as sharp carbon isotope excursions (Bond and Grasby, 2017; Wignall, 2015).

Yet critical questions persist. Why have some large igneous province eruptions been associated with mass extinctions while others have not? Why does the magnitude of extinction vary dramatically across events, even

when the apparent intensity of the external perturbation seems similar? These observations suggest that the impact of external perturbations is mediated by the internal state of the biosphere at the time of disturbance, a factor that traditional extinction research has often treated as secondary to the trigger itself.

1.3 Toward a Unified Framework

The central thesis of this paper is that species radiations and mass extinctions are not merely two ends of a spectrum but are two manifestations of the same underlying dynamical process: the crossing of critical thresholds in a complex adaptive system. I propose that the global ecosystem can be understood as a high-dimensional dynamical system characterized by an ecological landscape whose topology is shaped by the interplay between environmental conditions, evolutionary innovations, and the network structure of biotic interactions. Radiations correspond to the system crossing an innovation threshold, driven by the accumulation of evolutionary potential and the availability of unoccupied niche space. Mass extinctions correspond to the system crossing a collapse threshold, driven by external perturbations that overwhelm the system resilience. In this view, the key determinants of both phenomena are the same set of system-level variables: connectivity, redundancy, and the strength of environmental forcing.

This paper develops this theoretical framework in four stages: (1) Provide a comprehensive review of the existing literature on the causes of evolutionary radiations and mass extinctions, identifying both the insights and the limitations of current approaches. (2) Present a unified theoretical model that incorporates the key mechanisms identified in the literature into a coherent mathematical framework based on stochastic differential equations and network percolation theory. (3) Describe a suite of methodological innovations, including deep learning-based paleoecological network reconstruction and multi-proxy early warning signal detection, designed to test the predictions of the unified model against the fossil record. (4) Discuss the implications of this framework for understanding the dynamics of contemporary biodiversity loss and the potential for a sixth mass extinction.

2 Theoretical Dilemma: From Single Causes to Complex Systems

2.1 Causal Hypotheses for Evolutionary Radiations

2.1.1 Environmental Triggers

A long-standing hypothesis attributes the Cambrian explosion to a significant increase in atmospheric and oceanic oxygen concentrations. The physiological demands of large, metabolically active animals require oxygen levels above a certain threshold, and geochemical proxies suggest that Neoproterozoic oxygen levels may have crossed this threshold close to the Ediacaran-Cambrian boundary (Canfield et al., 2007; Lyons, Reinhard and Planavsky, 2014). Sperling et al. (2013) demonstrated that the oxygen requirements of modern carnivorous bilaterians are substantially higher than those of simpler organisms, suggesting that the rise of oxygen was a necessary precondition for the evolution of complex animal ecosystems. However, subsequent work has complicated this narrative. Mills et al. (2014) argued that the oxygen requirements of early animals may have been lower than previously assumed, and that oxygen levels sufficient to support bilaterian life may have existed long before the Cambrian radiation.

Nutrient availability represents another class of environmental trigger. The erosion associated with the Great Unconformity, a global episode of enhanced continental weathering, may have delivered large quantities of phosphorus, calcium, and other essential nutrients to the oceans, fueling primary productivity and enabling the expansion of metazoan ecosystems (Peters and Gaines, 2012). Brasier and Lindsay (2001) proposed that increased nutrient flux from continental weathering, combined with changes in ocean circulation, could have driven a cascade of ecological changes culminating in the Cambrian radiation. The phosphorus enrichment of

the environment would cause excess primary production, but it is neither directly linked with diversity nor disparity (Zhang et al., 2014).

Seawater chemistry also changed dramatically across the Ediacaran-Cambrian transition. The increasing availability of calcium ions, driven by the weathering of continental crust, may have facilitated the evolution of biomineralization, enabling the construction of skeletons and shells that are characteristic of Cambrian faunas (Brennan, Lowenstein and Horita, 2004). The decline of oceanic salinity, associated with the sequestration of salt in evaporite basins, may have reduced osmotic stress on early animals (Knauth, 2005).

2.1.2 Developmental and Genomic Innovations

The discovery of the Hox gene complex, a highly conserved set of transcription factors that regulate anterior-posterior patterning in bilaterian animals, provided a powerful developmental explanation for the Cambrian explosion. The duplication and diversification of Hox genes in the bilaterian stem lineage may have enabled the evolution of distinct regional identities along the body axis, facilitating the construction of diverse body plans from a relatively simple genetic toolkit (Carroll, 2006; Erwin and Davidson, 2002). Valentine (2006) argued that the evolution of developmental mechanisms enabling pattern formation, those processes that delay the specification of cells and thereby allow for growth, was one major innovation that allowed for the evolution of distinct macroscopic body plans by the end of the Precambrian.

However, molecular clock analyses have complicated the developmental trigger hypothesis by suggesting that the bilaterian radiation may have significantly predated its morphological expression in the fossil record. Douzery et al. (2004) estimated that the last common ancestor of bilaterians lived between 650 and 700 million years ago, well before the Cambrian. This implies that the genetic and developmental machinery for building complex animals existed long before those animals actually appeared in the fossil record, suggesting that environmental or ecological factors, rather than genomic ones, were the proximate triggers for the Cambrian explosion (Erwin et al., 2011).

The evolution of macrophagy, the ability to consume large food items, has been proposed as a key ecological trigger. The advent of benthic predation would have initiated an evolutionary arms race, driving the evolution of larger body sizes, defensive skeletons, and increased mobility, all of which are characteristic of Cambrian faunas (Marshall, 2006). The evolution of macrophagy near the end of the Marinoan glacial interval may have been the inevitable outcome of earlier developmental innovations combined with changing ecological conditions. Benthic predation pressures also resulted in the evolution of mesozooplankton, which irrevocably linked the pelagos with the benthos, effectively establishing the Phanerozoic ocean.

2.1.3 Ecological Opportunity and Adaptive Radiation

Simpson (1984, 1953) introduced the concept of the adaptive zone: a set of ecological niches that a lineage can occupy given its morphological and physiological characteristics. According to Simpsonian theory, adaptive radiations occur when a lineage enters a new adaptive zone, either through the evolution of a key innovation, the extinction of competitors, or the colonization of a new geographic region. This ecological opportunity releases the lineage from the diversity-dependent constraints that typically limit diversification, resulting in a burst of speciation as the lineage fills the available niche space.

This framework has been successfully applied to a wide range of adaptive radiations across the tree of life. Grant and Grant (2011) documented the adaptive radiation of Darwin finches in the Galápagos Islands, demonstrating how ecological opportunity, driven by variation in food availability, can drive rapid morphological and ecological diversification. Losos (2011) showed that the adaptive radiation of Anolis lizards in the Caribbean was shaped by the availability of distinct microhabitats, with similar ecomorphs evolving convergently on different islands. The Malagasy vanga radiation provides a more recent example, with

exceptional ecomorphological diversity evolving along multiple independent trait axes, mainly driven by a late expansion in niche space due to key innovations (Reddy et al., 2012).

The application of this framework to the Cambrian explosion has been more challenging. The Cambrian radiation involved the simultaneous diversification of multiple phyla across very different ecological contexts, making it difficult to attribute to a single ecological opportunity. However, the post-extinction context of the Ediacaran-Cambrian transition, following the disappearance of the distinctive Ediacaran biota, may have created an unprecedented ecological vacuum that multiple lineages could exploit simultaneously (Darroch, Sperling and Boag, 2015).

2.2 Causal Hypotheses for Mass Extinctions

2.2.1 Bolide Impact

The discovery of an iridium anomaly at the Cretaceous-Paleogene boundary by Alvarez et al. (1980) revolutionized the study of mass extinctions, providing the first compelling evidence for an extraterrestrial cause. The subsequent identification of the Chicxulub impact crater in the Yucatán Peninsula, Mexico, confirmed that a large asteroid approximately 10 kilometers in diameter struck the Earth approximately 66 million years ago (Schulte et al., 2010). The Chicxulub impact is widely regarded as the primary cause of the Cretaceous-Paleogene mass extinction, which eliminated approximately 76% of all species, including all non-avian dinosaurs (Morgan et al., 2022).

The kill mechanisms associated with the Chicxulub impact are multifaceted. The impact would have injected enormous quantities of dust, soot, and sulfate aerosols into the atmosphere, blocking sunlight and causing a global impact winter lasting months to years (Vellekoop et al., 2014). The cessation of photosynthesis would have collapsed primary productivity in both marine and terrestrial ecosystems, triggering a cascade of secondary extinctions throughout food webs. Sulfuric acid rain, generated from the vaporization of sulfate-rich target rocks at the impact site, would have acidified terrestrial and freshwater environments (Ohno et al., 2014). Wildfires ignited by the thermal radiation of re-entering ejecta would have consumed large portions of terrestrial biomass (Robertson et al., 2013).

Despite the strength of the evidence linking the Chicxulub impact to the end-Cretaceous mass extinction, the bolide impact hypothesis faces significant challenges when extended to other extinction events. No impact craters comparable in size and age to other major extinction boundaries have been identified. The search for iridium anomalies and shocked quartz at the Permian-Triassic, Triassic-Jurassic, and other boundaries has yielded ambiguous or negative results. Claims of periodicity in the extinction record, which were used to argue for a common extraterrestrial trigger for all mass extinctions, have been contested on statistical grounds (Bailer-Jones, 2009).

2.2.2 Large Igneous Province Eruptions

The association between large igneous province eruptions and mass extinctions has emerged as one of the most robust patterns in Earth history. The end-Permian mass extinction coincides temporally with the emplacement of the Siberian Traps, the largest continental flood basalt province known from the geological record (Burgess et al., 2014; Svensen et al., 2009). The end-Triassic mass extinction is closely associated with the Central Atlantic Magmatic Province, whose emplacement accompanied the initial breakup of Pangaea (Whiteside et al., 2010; Davies et al., 2017). The Cretaceous-Paleogene mass extinction, although primarily attributed to the Chicxulub impact, also coincides with the eruption of the Deccan Traps in India, leading some researchers to argue that the extinction resulted from a combination of impact and volcanic drivers (Keller, 2014; Schoene et al., 2019).

The kill mechanisms associated with large igneous province eruptions are diverse and often synergistic. The release of carbon dioxide from magmatic degassing and from the thermal metamorphism of organic-rich

sediments drives global warming and ocean acidification (Svensen et al., 2009). The release of sulfur dioxide generates sulfate aerosols that cause short-term cooling episodes, alternating with longer-term warming driven by CO_2 accumulation. Halogen emissions can deplete stratospheric ozone, increasing ultraviolet radiation at the surface (Black, Elkins-Tanton and Rowe, 2012). The release of toxic metals, including mercury, lead, and nickel, can poison marine and terrestrial ecosystems (Grasby et al., 2019).

The recent geochemical study confirming the connection between Siberian Traps flood basalt volcanism, marine anoxia, and the end-Permian mass extinction has provided a specific kill mechanism. Nickel isotopes link Siberian Traps aerosol particles to the end-Permian mass extinction, demonstrating that nickel-rich particles from the volcanic emissions were deposited in marine sediments, where they would have been toxic to marine life (Li et al., 2021). Global changes of atmospheric CO_2 and paleotemperature, both icehouse and greenhouse conditions, oceanic acidification, sea-level changes, and anoxia triggered by massive volcanisms were the most plausible causes of the past extinctions (Shen and Zhang, 2017).

2.2.3 Marine Anoxia and Biogeochemical Perturbations

Widespread marine anoxia, the depletion of dissolved oxygen in ocean waters, has been implicated in several mass extinctions, particularly the Late Devonian and end-Permian events. The expansion of land plants during the Late Devonian may have contributed to marine anoxia by increasing the terrestrial release of the nutrient phosphorus, which fueled eutrophication and oxygen depletion in coastal waters (Smart et al., 2023). Oceanic anoxia and euxinia, the presence of hydrogen sulfide in the water column, have been argued as an important cause of the Late Devonian mass extinction (Bond and Wignall, 2008).

The end-Permian mass extinction is associated with the most severe episode of marine anoxia in the Phanerozoic. Geochemical proxies indicate that oxygen depletion extended from the deep ocean into shallow shelf environments, eliminating the habitable zone for most marine organisms (Wignall and Twitchett, 1996). The expansion of euxinic conditions, characterized by free hydrogen sulfide in the water column, would have been toxic to aerobic organisms and may have contributed to the selective extinction of marine invertebrates (Grice et al., 2005).

Ocean acidification represents another important kill mechanism. The rapid injection of CO_2 into the atmosphere, whether from volcanic degassing or from other sources, drives a decrease in ocean pH that disproportionately affects calcifying organisms (Wu and Zhang, 2012). The selective extinction of heavily calcified marine organisms at the end-Permian and end-Triassic boundaries is consistent with ocean acidification as a proximal kill mechanism (Kiessling and Simpson, 2011; Hautmann et al., 2008).

2.2.4 The Multi-Causal Consensus

Every mass extinction has both an ultimate cause, that is the trigger that leads to various climato-environmental changes, and one or more proximate causes, the specific climato-environmental changes that result in elevated biotic mortality (Algeo and Shen, 2024). With regard to ultimate causes, strong cases can be made that bolide impacts, large igneous province eruptions, and bio-evolutionary events have each triggered one or more of the Phanerozoic Big Five mass extinctions. With regard to proximate mechanisms, most extinctions are related to either carbon-release or carbon-burial processes, the former being associated with climatic warming, ocean acidification, reduced marine productivity, and lower carbonate $\delta^{13}C$ values, and the latter with climatic cooling, increased marine productivity, and higher carbonate $\delta^{13}C$ values (Algeo and Shen, 2024).

Among the Big Five mass extinctions, the end-Cretaceous biocrisis is an example of a bolide-triggered carbon-release event, the end-Permian and end-Triassic biocrises are examples of LIP-triggered carbon-release events, and the Late Ordovician and Late Devonian biocrises are examples of bio-evolution-triggered carbon-burial events (Algeo and Shen, 2024). This classification provides a useful framework for organizing the

diversity of extinction triggers and mechanisms, yet it does not fully address the question of why the magnitude and selectivity of extinction vary so dramatically across events.

The consensus that has emerged from decades of extinction research is that mass extinctions are typically multi-causal phenomena, resulting from the convergence of multiple environmental stresses operating at different spatial and temporal scales (Bond and Grasby, 2017). The Siberian Traps volcanism, for example, would have driven global warming, ocean acidification, marine anoxia, toxic metal poisoning, and ozone depletion simultaneously, creating a lethal combination that no single stress could achieve alone. The combination of lowering of sea level and glacially driven cooling are likely driving agents for the Ordovician mass extinction (Brenchley et al., 2001).

2.3 Theoretical Frameworks for Macroevolutionary Dynamics

2.3.1 The Red Queen and Court Jester Hypotheses

The Red Queen hypothesis, introduced by Van Valen (1973), proposes that species must constantly evolve to maintain their fitness relative to co-evolving competitors, predators, and parasites. In this view, extinction is driven primarily by biotic interactions, and the probability of extinction is independent of a lineage age. The Court Jester hypothesis, in contrast, emphasizes the role of abiotic environmental changes, such as climate fluctuations, sea-level changes, and tectonic events, as the primary drivers of extinction and diversification (Barnosky, 2001).

Both hypotheses have received empirical support from different contexts. The Red Queen hypothesis is consistent with the pattern of constant extinction risk observed in many fossil lineages and with the arms race dynamics documented in predator-prey and host-parasite systems. The Court Jester hypothesis is consistent with the correlation between extinction rates and environmental perturbations observed at mass extinction boundaries. The growing recognition is that both mechanisms operate simultaneously, with their relative importance varying across temporal and spatial scales (Benton, 2009). The advent of pervasive carnivory, made possible by oxygenation, is likely to have been a major trigger for the Cambrian explosion, combining elements of both Red Queen and Court Jester dynamics.

2.3.2 Punctuated Equilibrium

Eldredge and Gould (1972) proposed the theory of punctuated equilibrium as an alternative to the gradualistic model of evolution that had dominated paleontological thinking. According to punctuated equilibrium, most morphological change occurs during brief speciation events, with species exhibiting relative stasis throughout the majority of their duration. The theory was based on the observation that the fossil record often shows species appearing suddenly and persisting with little morphological change until their disappearance.

Punctuated equilibrium has important implications for understanding macroevolutionary dynamics. If most evolutionary change is concentrated in speciation events, then the rate of evolution is largely determined by the rate of speciation, which in turn may be influenced by environmental and ecological factors. The punctuational pattern also implies that evolutionary radiations can occur rapidly when conditions are favorable, consistent with the pattern observed in the Cambrian explosion and other major radiations. With the model of punctuated equilibria, an unbiased distribution of evolutionary tempos can be established by treating stasis as data and by recording the pattern of change for all species in an assemblage (Gould and Eldredge, 1977).

2.3.3 Self-Organized Criticality in Macroevolution

Bak and Sneppen (1993) proposed a model of macroevolution based on the concept of self-organized criticality (SOC). In their model, species are arranged on a one-dimensional lattice, with each species assigned a fitness value. The species with the lowest fitness is replaced by a new species, and its neighbors are assigned new fitness values, representing the co-evolutionary consequences of extinction. This simple model generates

avalanches of extinctions whose size distribution follows a power law (Zhang, 2012a, 2016b. 2018, 2023), consistent with the pattern observed in the fossil record.

The SOC model provides a compelling explanation for several features of the macroevolutionary record, including the power-law distribution of extinction event magnitudes, the lack of periodicity in extinction events, and the alternation between periods of stasis and rapid change that characterizes punctuated equilibrium (Sneppen et al., 1995). The fossil record of life has been shown to provide evidence for scaling laws in both time series and in the distribution of extinction event magnitudes (Newman and Palmer, 2003).

However, the SOC model has significant limitations. The model treats extinction as a purely endogenous process, driven by internal co-evolutionary dynamics, and does not adequately account for the role of external perturbations in driving mass extinctions. Neither are speciations and extinctions in real biological macroevolution known to contain any diverging distributions, or self-organization (Zhang, 2016b) towards any critical state (Kärenlampi, 2015). The model also does not distinguish between background extinction and mass extinction, treating all extinction events as part of a continuous distribution.

2.3.4 Network Models of Macroevolution

The recognition that species do not exist in isolation but are embedded in complex networks of ecological interactions (Zhang, 2011, 2012a, 2016b, 2018, 2021) has led to the development of network-based models of macroevolution. These models incorporate the effects of species interactions on extinction risk, allowing for the possibility that the extinction of one species can trigger a cascade of secondary extinctions throughout the network.

Dunne et al. (2008) reconstructed Cambrian food webs from the Burgess Shale and Chengjiang Lagerstätten, revealing that these early animal communities exhibited complex trophic structures including multiple trophic levels, omnivory, and indirect interactions. The complexity of early Cambrian food webs suggests that ecological interactions were already a significant factor shaping macroevolutionary dynamics during the Cambrian explosion.

Network theory provides a powerful framework for understanding extinction cascades. The extinction of a single species might cause another species to die out, which might drive a third species into extinction and so on, producing an avalanche that in principle could span the whole system (Newman and Palmer, 2003). The probability and magnitude of such cascades depend on the topology of the interaction network (Zhang, 2011, 2012a, 2016b, 2018), with highly connected, low-redundancy networks being more vulnerable to cascade-driven collapse than networks with high modularity and functional redundancy (Dunne and Williams, 2009; Zhang, 2012a, 2018).

A model for evolution and extinction incorporating the effects of interactions between species and the influences of abiotic environmental factors suggests that a possible mechanism for mass extinction is the coincidence of a large co-evolutionary avalanche in the ecosystem with a severe environmental disturbance (Newman, 1997). This insight points toward the need for a theoretical framework that integrates both endogenous network dynamics (Zhang, 2012b, 2015) and exogenous environmental forcing.

2.3.5 Critical Transitions and Tipping Points

The theory of critical transitions, developed primarily in the context of ecosystem ecology and climate science, provides a formal mathematical framework for understanding abrupt regime shifts in complex dynamical systems (Scheffer et al., 2001, 2009, 2012; Scheffer, 2009). According to this theory, many complex systems exhibit alternative stable states separated by critical thresholds. When a system approaches such a threshold, its dynamics exhibit characteristic early warning signals, including critical slowing down, increased variance, and increased autocorrelation (Zhang, 2016b).

Critical slowing down, measured as increased autocorrelation, can be mathematically shown to be a hallmark of tipping points (Dakos et al., 2008). This provides independent empirical evidence for the idea that past abrupt shifts were associated with the passing of critical thresholds, and could be used as a universal early warning signal for upcoming catastrophic change (Scheffer et al., 2009).

The application of critical transition theory to paleobiological data has been limited but promising. Early-warning signals for Cenozoic climate transitions have been detected in paleoclimate time series, demonstrating that the statistical signatures of critical transitions can be identified in the geological record (Dakos et al., 2008). The extension of this approach to biological time series, including diversity curves and fossil occurrence data, holds significant potential for understanding the dynamics of past extinctions and radiations (Zhang, 2017).

2.3.6 Adaptive Landscape Theory

Wright (1932) introduced the concept of the adaptive landscape, a metaphorical representation of the relationship between genotype or phenotype and fitness. The adaptive landscape depicts fitness as a function of one or more traits, with peaks representing high-fitness combinations and valleys representing low-fitness combinations (Zhang, 2016b). Populations evolve by climbing local peaks under the influence of natural selection, but may become trapped on suboptimal peaks if the intervening valleys are too deep.

Simpson (1984, 1953) adapted the adaptive landscape concept for macroevolution, arguing that major evolutionary transitions involve shifts from one adaptive zone to another across regions of low fitness. The topology of the landscape itself may change over time as environmental conditions change and as new adaptations evolve. The status of theoretical work has been reviewed and the importance of models for peak movement on stationary, unchanging landscapes has been emphasized, with a focus on the evolution of the landscape itself (Arnold, Pfrender and Jones, 2001).

The adaptive landscape provides a natural framework for understanding both radiations and extinctions. Radiations correspond to populations discovering and occupying new adaptive peaks, while extinctions correspond to the disappearance of peaks as environmental conditions change. The key challenge is to operationalize this metaphorical framework into a quantitative, testable model. The topology of evolutionary novelty and innovation in macroevolution can be understood as the creation of new adaptive peaks through the evolution of key innovations.

2.4 The Gap: Toward an Integrated Dynamics

The research above reveals a fundamental gap in current theoretical understanding. Research on evolutionary radiations has identified a rich set of causal mechanisms but has not developed a unified framework that explains why radiations occur with such dramatic synchronicity across diverse clades. Research on mass extinctions has documented the environmental triggers and proximal kill mechanisms in detail but has not adequately explained why the magnitude of extinction varies so dramatically. The theoretical frameworks of self-organized criticality, network dynamics, and critical transitions each capture important aspects of the problem, but they have largely been developed in isolation from one another and from the empirical literature on specific extinction and radiation events.

What we needed is a theoretical framework that unifies these disparate strands into a coherent model of macroevolutionary dynamics. Such a framework must incorporate the role of external perturbations, the internal dynamics of ecological networks, the evolutionary generation of novelty, and the systemic properties that determine whether a given perturbation triggers a mass extinction or a modest turnover. In the following I will present such a framework, drawing on the concepts of ecological landscapes, critical transitions, and network percolation theory.

3 Theoretical Innovation: A Unified Critical Transition Model for Macroevolutionary Dynamics

3.1 The Ecological Landscape as a State Space

I conceptualize the global ecosystem as a high-dimensional dynamical system whose state at any given time can be described by a set of macroscopic variables: total taxonomic diversity, functional diversity, network connectivity, and ecosystem productivity. The dynamics of this system can be visualized as the movement of a point in a state space whose topography is determined by the interplay between environmental conditions, biotic interactions, and evolutionary innovations (Fig. 1).

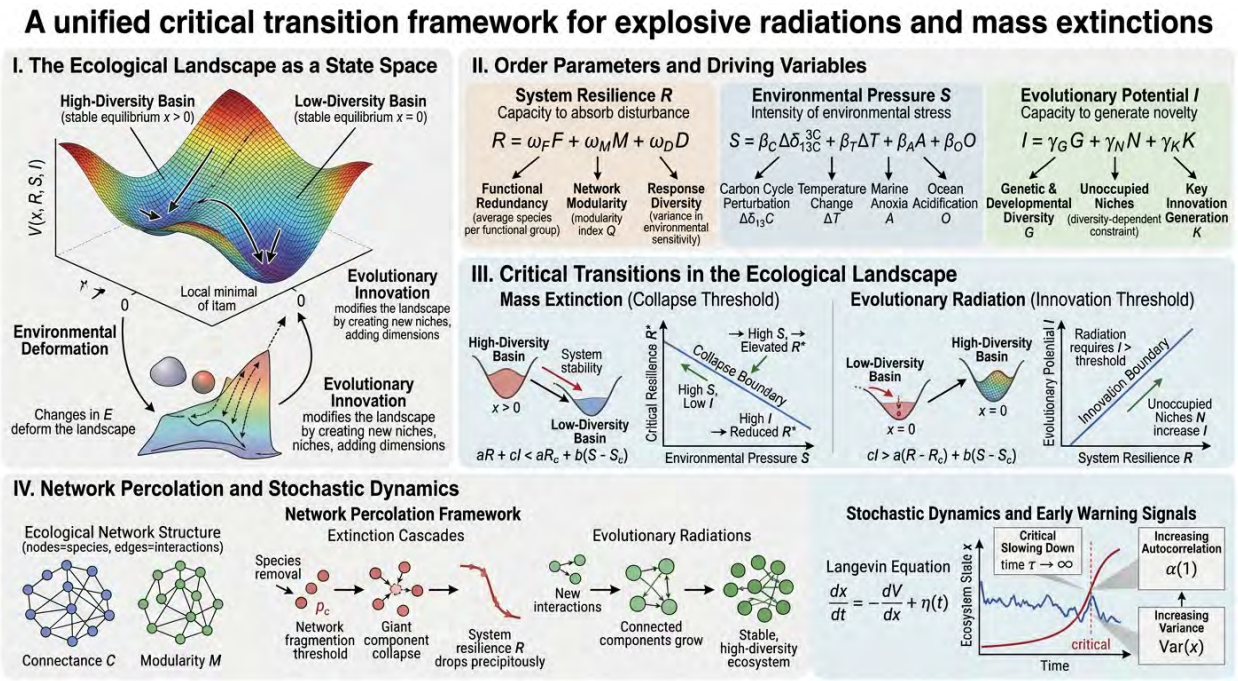

Fig. 1 Schematic diagram of the unified critical transition framework for explosive radiations and mass extinctions.

Formally, I define the ecological landscape as a potential function $V(x, E, I)$ that maps the system state vector x onto a measure of system stability or persistence, given environmental conditions E and the set of evolutionary innovations I available to the biota. The state vector x includes variables such as the number of species, the distribution of functional traits, and the structure of the interaction network (Zhang, 2015, 2016b, 2018). The system evolves by moving toward local minima of V, which correspond to stable configurations of the ecosystem.

The landscape is not static. Changes in environmental conditions E deform the landscape, potentially eliminating existing minima or creating new ones. Evolutionary innovations I modify the landscape by creating new niches that populations can occupy, effectively adding new dimensions to the state space. The interplay between environmental deformation and evolutionary innovation generates the dynamics that I observe as radiations and extinctions.

3.2 Defining Order Parameters and Driving Variables

To operationalize the landscape model, I define three order parameters that collectively describe the state of the system and its proximity to critical thresholds. These parameters are chosen to capture the key dimensions of system behavior identified in the previous review: the capacity of the system to absorb perturbations, the intensity of environmental stress, and the potential for evolutionary innovation.

3.2.1 System Resilience *R*

System resilience *R* measures the capacity of the ecosystem to absorb disturbance while maintaining its essential structure and function. Based on the ecological resilience literature (Holling, 1973; Folke et al., 2004), I define *R* as a composite variable incorporating three components: functional redundancy, network modularity, and response diversity.

Functional redundancy *F* quantifies the degree to which multiple species perform similar ecological functions. Communities with high functional redundancy are more resilient because the loss of any single species can be compensated by other species performing the same function. I define functional redundancy as the average number of species per functional group, weighted by the importance of each group to ecosystem function.

Network modularity *M* quantifies the degree to which the ecological network is partitioned into semi-independent modules with dense internal connections and sparse connections between modules (Zhang, 2016a; Zhang and Li, 2016). Modular networks are more resilient because perturbations are less likely to propagate from one module to another. I define network modularity using the standard modularity index *Q* from network theory (Newman, 2006).

Response diversity *D* quantifies the diversity of responses to environmental change among species within the same functional group. Communities with high response diversity are more resilient because environmental changes that negatively affect one species may not affect other species performing the same function. I define response diversity as the variance in environmental sensitivity among species within each functional group.

The system resilience *R* is then defined as:

$$R = \alpha_F F + \alpha_M M + \alpha_D D$$

where α_F, α_M, and α_D are weighting coefficients that may be estimated from empirical data or determined from mechanistic models.

3.2.2 Environmental Pressure *S*

Environmental pressure *S* measures the intensity of environmental stress acting on the ecosystem. Following the classification of mass extinction mechanisms developed by Algeo and Shen (2024), I define *S* as a composite variable incorporating: the rate of carbon cycle perturbation, measured by the magnitude and rate of change of $\delta^{13}C$; the rate of temperature change; the extent of marine anoxia, and the magnitude of ocean acidification.

The environmental pressure *S* can be expressed as:

$$S = \beta_C \left|\frac{d\delta^{13}C}{dt}\right| + \beta_T \left|\frac{dT}{dt}\right| + \beta_A A + \beta_O O$$

where *A* represents the extent of marine anoxia, *O* represents the magnitude of ocean acidification, and the β coefficients are weighting parameters.

3.2.3 Evolutionary Potential *I*

Evolutionary potential *I* measures the capacity of the biota to generate evolutionary novelty in response to ecological opportunity. I define *I* as a composite variable incorporating: the standing genetic and developmental diversity available to lineages, the number of unoccupied niches, and the rate of key innovation generation.

The evolutionary potential I can be expressed as:

$$I = \gamma_G G + \gamma_N N + \gamma_K K$$

where G represents genomic and developmental complexity, N represents the number of unoccupied niches, and K represents the rate of key innovation emergence.

The number of unoccupied niches N is a particularly important variable. Following the theory of diversity-dependent diversification, the rate of speciation declines as niches are filled (Rabosky and Hurlbert, 2015). Mass extinctions create unoccupied niches by eliminating incumbent species, thereby increasing N and creating the conditions for subsequent radiations. Conversely, during periods of high diversity, niche space is saturated and evolutionary potential is low despite high standing genetic diversity.

3.3 The Landscape Potential Function

I propose a potential function (Zhang, 2016) for the ecological landscape that captures the interplay between the order parameters:

$$V(x, R, S, I) = a(R - R_c)x^2 + b(S - S_c)x^2 - cIx^2 + dx^4$$

Here, x represents a generalized measure of ecosystem state, such as total diversity or functional complexity. The parameter R_c is the critical resilience threshold below which the system becomes vulnerable to collapse. The parameter S_c is the critical environmental pressure threshold above which the system is driven toward collapse. The coefficients a, b, c, and d are positive constants that determine the shape of the landscape.

The first term $a(R - R_c)x^2$ represents the stabilizing effect of system resilience. When $R > R_c$, this term is positive and contributes to a single stable equilibrium at $x = 0$, representing a high-diversity state. When $R < R_c$, this term becomes negative, destabilizing the high-diversity state and potentially leading to a transition to a low-diversity state.

The second term $b(S - S_c)x^2$ represents the destabilizing effect of environmental pressure. When $S > S_c$, this term is positive and contributes to destabilization. When $S < S_c$, this term is negative and contributes to stabilization.

The third term $-cIx^2$ represents the diversifying effect of evolutionary potential. This term is always negative, contributing to the creation of new stable states at non-zero values of x, representing high-diversity configurations.

The fourth term dx^4 ensures that the potential remains bounded and that stable states exist at finite values of x.

The minima of V with respect to x determine the stable states of the ecosystem. Setting $dV/dx = 0$ yields:

$$x[2a(R - R_c) + 2b(S - S_c) - 2cI + 4dx^2] = 0$$

The solutions are x and:

$$x^2 = (cI - a(R - R_c) - b(S - S_c))/(2d)$$

The state x represents a low-diversity state, such as the aftermath of a mass extinction. The non-zero solution represents a high-diversity state. The stability of these states depends on the values of the order parameters.

3.4 Critical Transitions in the Ecological Landscape

3.4.1 The Collapse Threshold: Conditions for Mass Extinction

A mass extinction corresponds to the system crossing from a high-diversity basin of attraction to a low-diversity basin. This transition occurs when the high-diversity state loses stability, which happens when the argument of the square root in the non-zero solution becomes negative:

$$cI - a(R - R_c) - b(S - S_c) < 0$$

Rearranging:

$$a\,R + c\,I < aR_c + b(S - S_c)$$

This inequality defines the collapse boundary in the parameter space. For given values of environmental pressure S and evolutionary potential I, there is a critical resilience R^* below which the high-diversity state becomes unstable:

$$R^* = R_c + (b/a)(S - S_c) - (c/a)I$$

When S is high and I is low, R^* is elevated, meaning that the system requires higher resilience to avoid collapse. When I is high, R^* is reduced, meaning that even a system with low resilience may maintain diversity if evolutionary potential is sufficient to generate new adaptations.

This formulation captures a key insight from the empirical research: the magnitude of extinction depends not only on the intensity of the external perturbation but also on the pre-existing state of the ecosystem. A system with low resilience due to low functional redundancy or high network connectivity may suffer catastrophic collapse even when faced with moderate environmental pressure. Conversely, a highly resilient system with high functional redundancy and modular network structure may withstand substantial environmental perturbation without undergoing a mass extinction.

3.4.2 The Innovation Threshold: Conditions for Evolutionary Radiation

A radiation corresponds to the system crossing from a low-diversity basin to a high-diversity basin. This transition occurs when the low-diversity state $x = 0$ loses stability and a new stable high-diversity state emerges. From the stability analysis of the potential function, the low-diversity state becomes unstable when:

$$a(R - R_c) + b(S - S_c) - cI < 0$$

Rearranging:

$$cI > a(R - R_c) + b(S - S_c)$$

This inequality defines the innovation boundary. Radiation occurs when evolutionary potential I exceeds a threshold that depends on the current resilience and environmental pressure.

An important implication of this formulation is that radiation requires more than just the availability of empty niche space. Even after a mass extinction has cleared niches, radiation will not occur unless evolutionary potential is sufficient to generate the adaptations required to occupy those niches. This explains the observation that recovery from mass extinctions can be delayed, sometimes by millions of years, and that the tempo of recovery varies across different extinction events (Erwin, 1998; Chen and Benton, 2012).

The presence of unoccupied niches, represented by a decrease in the diversity-dependent constraint on I, increases evolutionary potential by providing ecological opportunity. However, the genetic and developmental machinery for exploiting that opportunity must also be present. The evolution of key innovations, such as the Hox gene complex in the Cambrian or the mammalian middle ear in the Triassic, can increase I by opening new regions of niche space.

3.5 Network Percolation and the Connectivity Threshold

The landscape model described above treats the ecosystem as a homogeneous system characterized by macroscopic order parameters. To capture the specific mechanisms by which extinctions and radiations propagate through ecological networks, I incorporate a network percolation framework.

3.5.1 Ecological Network Structure and Stability

Consider an ecological network consisting of N species connected by trophic and non-trophic interactions. The network can be represented as a graph in which nodes represent species and edges represent interactions (Zhang, 2011, 2012a, 2016b, 2018, 2023; Shams and Khansari, 2014; Zhang and Zhang, 2019). The connectance C of the network is defined as the fraction of possible edges that are actually present:

$$C = L/ (N(N\text{-}1)/2)$$

where L is the number of edges in the network.

May (1972) demonstrated that the stability of random ecological networks depends on the relationship between connectance, species richness, and interaction strength. Specifically, a randomly connected system is stable if:

$$\sigma (SC)^{1/2} < d$$

where σ is the standard deviation of interaction strengths, S is the number of species, C is connectance, and d is the strength of density-dependent self-regulation. This result implies that complexity, measured by the product of species richness and connectance, can be destabilizing when interaction strengths are high.

However, subsequent work has shown that the relationship between complexity and stability is more nuanced than May original analysis suggested. Real ecological networks exhibit non-random structural features, including modularity, nestedness, and degree heterogeneity (Zhang, 2012a, 2016b, 2018), that can enhance stability even at high levels of complexity. Positive complexity-stability relations have been demonstrated in food web models without foraging adaptation (Kondoh, 2003). Increasing network complexity can lead to decreasing stability in some models, a result that is contradictory to earlier empirical findings (Allesina and Tang, 2012).

3.5.2 Percolation Theory and Extinction Cascades

Percolation theory provides a mathematical framework for understanding how the removal of nodes from a network affects its global connectivity (Zhang, 2016a, Zhang and Li, 2016). In a random network, there exists a critical occupation probability p_c above which a giant connected component spanning a finite fraction of the network exists. Below p_c, the network fragments into small, disconnected clusters.

The analogy to extinction is direct. The removal of species from an ecological network, whether through direct environmental stress or through co-extinction, can be modeled as a percolation process. When the fraction of surviving species falls below a critical threshold, the giant component of the ecological network collapses, and the ecosystem fragments into isolated modules (Zhang, 2012a, 2018). This fragmentation may

itself trigger further extinctions, as species that depend on interactions with now-isolated species lose access to essential resources.

The critical threshold for percolation in a random network with arbitrary degree distribution is given by (Molloy and Reed, 1995):

$$\frac{\langle k^2 \rangle}{\langle k \rangle} = 2$$

where $\langle k \rangle$ and $\langle k^2 \rangle$ are the first and second moments of the degree distribution. Networks with highly heterogeneous degree distributions, characterized by a few highly connected hub nodes, are more vulnerable to targeted removal of hubs than to random removal, but more resilient to random removal than homogeneous networks (Albert et al., 2000).

3.5.3 Integrating Network and Landscape Dynamics

I integrate the network percolation framework with the landscape model by expressing the system resilience R in terms of network properties:

$$R = R_0 \, f(\frac{\langle k^2 \rangle}{\langle k \rangle}, M, F)$$

where R_0 is a baseline resilience, f is a function that increases with modularity M and functional redundancy F, and decreases as the ratio $\frac{\langle k^2 \rangle}{\langle k \rangle}$ increases, reflecting the vulnerability of scale-free networks to targeted perturbations.

The collapse threshold condition derived from the landscape model can then be expressed in terms of network properties. When the fraction of species surviving an environmental perturbation falls below the percolation threshold, the ecological network fragments, system resilience drops precipitously, and the ecosystem undergoes a transition from a high-diversity to a low-diversity state in the landscape.

Conversely, evolutionary radiations can be understood as the reverse process: the establishment of new interactions among species creates connected components in niche space that grow until they percolate, at which point a stable, high-diversity ecosystem emerges from a previously fragmented state.

3.6 Stochastic Dynamics and the Role of Noise

The deterministic landscape model provides insight into the conditions under which critical transitions occur, but real ecosystems are subject to stochastic fluctuations at multiple scales. I incorporate stochasticity by modeling the ecosystem state as a diffusion process in the ecological landscape.

The stochastic dynamics of the ecosystem state x can be described by a Langevin equation:

$$dx/dt = - dV/dx + \sigma\eta(t)$$

where $\eta(t)$ is a Gaussian white noise process with zero mean and unit variance, and σ is the noise intensity.

The presence of noise means that transitions between basins can occur even when the deterministic conditions for transition are not met, through the mechanism of noise-induced escape. The rate of noise-induced transitions is given by the Kramers escape rate (Kramers, 1940):

$$r \propto e^{-\frac{\Delta V}{\sigma^2}}$$

where ΔV is the height of the potential barrier separating the two basins. As the system approaches a critical threshold, ΔV decreases, and the escape rate increases dramatically.

This stochastic framework generates the early warning signals of critical transitions that have been documented in the theoretical and empirical literature. As the system approaches a bifurcation point, the curvature of the potential basin decreases, leading to critical slowing down: the relaxation time following perturbations increases, and the variance and autocorrelation of the state variable increase. These signals can be detected in time series data and used to anticipate impending transitions (Scheffer et al., 2009; Dakos et al., 2008).

For a system described by the stochastic differential equation above, the relaxation time τ following a small perturbation is given by:

$$\tau = 1/|V''(x_0)|$$

where $V''(x_0)$ is the second derivative of the potential at the equilibrium point x_0. As the system approaches a bifurcation, $V''(x_0) \to 0$, and $\tau \to \infty$, indicating critical slowing down.

The autocorrelation function for this process decays exponentially:

$$\rho(t) = e^{-\frac{t}{\tau}}$$

Thus, as τ increases, the autocorrelation at any fixed lag increases, providing a detectable early warning signal.

The variance of the state variable also increases near the bifurcation point:

$$\mathrm{Var}(x) = \frac{\sigma^2}{2|V''(x_0)|}$$

These statistical signatures, increasing autocorrelation and increasing variance, constitute the primary early warning signals for critical transitions in complex systems.

3.7 Synthesis: The Unified Dynamics

The theoretical framework developed above unifies the processes of evolutionary radiation and mass extinction within a single dynamical model. Both phenomena are manifestations of the same underlying dynamics: the crossing of critical thresholds in an ecological landscape whose topology is determined by the interplay between system resilience, environmental pressure, and evolutionary potential.

Mass extinctions occur when environmental pressure exceeds the critical threshold determined by system resilience, causing the high-diversity basin of attraction to disappear and the system to transition to a low-diversity state. The magnitude of extinction is determined not only by the intensity of the environmental perturbation but also by the pre-existing resilience of the ecosystem, which depends on network structure, functional redundancy, and the diversity of responses to environmental change.

Evolutionary radiations occur when evolutionary potential exceeds the critical threshold determined by system resilience and environmental pressure, causing a new high-diversity basin of attraction to emerge and the system to transition from a low-diversity to a high-diversity state. The timing and magnitude of radiations depend on the availability of ecological opportunity, the presence of developmental and genomic innovations,

and the structure of the ecological network that emerges as niches are filled.

The network percolation framework provides a mechanistic basis for understanding how extinctions and radiations propagate through ecological communities. The fragmentation of the interaction network below the percolation threshold represents the collapse of ecosystem function that characterizes mass extinctions, while the establishment of a percolating network of interactions represents the emergence of a stable, high-diversity ecosystem that characterizes radiations.

The stochastic extension of the model provides a framework for detecting early warning signals of impending transitions, opening the possibility of anticipating future biodiversity crises based on patterns observed in contemporary ecological data.

4 Methodological Innovation: Multi-Scale Detection and Simulation Framework

4.1 High-Resolution Paleoecological Network Reconstruction

Testing the predictions of the unified critical transition model requires detailed knowledge of ecological network structure across geological time, particularly during intervals immediately preceding and following major radiations and extinctions. Traditional approaches to reconstructing ancient food webs have relied on functional morphology, gut contents, and trace fossils to infer trophic relationships (Dunne et al., 2008). These methods are labor-intensive and limited to Lagerstätten with exceptional preservation, constraining their applicability across the full range of geological settings.

I propose a computational framework for reconstructing paleoecological networks that leverages recent advances in machine learning and statistical inference. The framework consists of three components: fossil co-occurrence analysis, functional trait inference, and network structure estimation.

4.1.1 Fossil Co-occurrence Analysis

The co-occurrence of fossil taxa in the same stratigraphic horizons provides information about potential ecological interactions. Bayesian network inference is used to estimate the probability of direct and indirect interactions based on patterns of co-occurrence, co-absence, and conditional occurrence across multiple localities and stratigraphic levels.

Given a matrix of fossil occurrences across localities and time bins, we may estimate the conditional dependence structure among taxa using Gaussian graphical models or more flexible non-parametric approaches. The resulting partial correlation network (Zhang, 2011, 2012a, 2018) represents a statistical approximation of the ecological interaction network, with edges indicating taxa whose occurrence patterns are correlated beyond what would be expected from shared environmental preferences alone.

4.1.2 Functional Trait Inference

Fossil morphology provides information about ecological function. Deep learning methods can be used to infer functional traits from fossil images and morphological measurements. Convolutional neural networks, trained on modern organisms with known ecological roles, can be applied to fossil specimens to predict traits such as feeding mode, mobility, and habitat preference (Du et al., 2024).

The integration of functional trait predictions with co-occurrence data enables the construction of more ecologically realistic networks. Taxa predicted to share similar functional traits are assigned to the same guilds, and interactions between guilds are inferred from co-occurrence patterns and functional constraints.

4.1.3 Network Structure Estimation

The final step in the reconstruction pipeline involves estimating the complete network structure from the combined co-occurrence and functional trait data. Exponential random graph models are used to identify the network configurations that best reproduce the observed patterns while accounting for structural constraints.

The reconstructed networks can be analyzed for properties relevant to the critical transition model, including connectance, modularity, degree distribution, and the presence of hub species. Changes in these properties across stratigraphic intervals provide empirical tests of the model predictions regarding network evolution near critical thresholds.

4.2 Early Warning Signal Detection in the Fossil Record

The stochastic model developed in the previous section predicts that ecosystems approaching critical thresholds should exhibit characteristic statistical signals: increasing autocorrelation, increasing variance, and critical slowing down. Detecting these signals in the fossil record requires careful treatment of the statistical properties of paleontological data, including irregular sampling, preservation bias, and taxonomic uncertainty.

4.2.1 Time Series Construction

Time series of biodiversity and ecosystem properties are constructed from fossil occurrence data compiled in the Paleobiology Database and other curated sources. These time series include: taxonomic diversity at multiple spatial and temporal scales, functional diversity estimated from morphological trait data, origination and extinction rates, and network properties such as connectance and modularity, estimated from reconstructed networks.

To account for sampling heterogeneity, use capture-mark-recapture methods to estimate true diversity from observed occurrence data, and use subsampling approaches to construct sampling-standardized diversity curves (Alroy, 2010).

4.2.2 Detection of Critical Slowing Down

The early warning signal methodology, developed by Dakos et al. (2008), is used to the paleontological time series. For each time series, compute the autocorrelation at lag-1, the standard deviation, and the skewness within a moving window. Increases in autocorrelation and variance, coupled with changes in skewness, are interpreted as indicators of critical slowing down.

To distinguish genuine early warning signals from spurious patterns arising from data artifacts, the surrogate data methods are used. Null distributions of the early warning indicators are generated by randomizing the time series while preserving their spectral properties, and the statistical significance of observed trends is assessed against these null distributions.

4.2.3 Multi-Proxy Integration

No single indicator provides a definitive signal of an approaching critical transition. I therefore integrate multiple proxies into a composite early warning index. The composite index is constructed using a weighted combination of individual indicators, with weights determined by the predictive performance of each indicator in simulated data with known transition points.

The application of this methodology to paleontological data from intervals preceding known mass extinctions provides empirical tests of the critical transition model. If the model is correct, I expect to observe significant increases in the composite early warning index in the intervals immediately preceding major extinction events.

4.3 Agent-Based Eco-Evolutionary Simulation

To complement the empirical analyses, I develop an agent-based simulation model that implements the core mechanisms of the unified critical transition framework (Appendix). The model simulates the evolution of a multi-species community on an explicitly represented ecological network, with environmental perturbations, evolutionary innovations, and extinction cascades all emerging from the interactions among individual agents.

4.3.1 Model Design

The simulation consists of a set of species, each characterized by a set of quantitative traits representing its ecological niche. Species interact through a food web in which each species is assigned a trophic level based

on its traits. The population dynamics of each species follow a Lotka-Volterra model with density-dependent growth and trophic interactions:

$$dN_i/dt = r_i N_i (1 - \frac{\sum_j \alpha_{ij} N_j}{K_i})$$

where N_i is the population size of species i, r_i is its intrinsic growth rate, α_{ij} is the interaction coefficient representing the effect of species j on species i, and K_i is the carrying capacity.

Evolution occurs through the generation of new species by speciation events, modeled as the splitting of an existing species into two daughter species with slightly modified traits. The rate of speciation is diversity-dependent, decreasing as niche space becomes saturated, consistent with empirical patterns (Rabosky and Hurlbert, 2015; Zhang, 2026a-b).

Environmental perturbations are imposed by modifying the carrying capacities of species as functions of time, with the magnitude and duration of perturbations varied systematically across simulation runs.

4.3.2 Calibration and Validation

The model is calibrated against empirical data from the Phanerozoic fossil record, including diversity trajectories, extinction and origination rates, and the distribution of extinction event magnitudes. Model parameters are estimated using approximate Bayesian computation, which identifies the parameter combinations that generate simulation outputs most closely matching the empirical patterns.

Validation is performed by comparing model predictions for intervals not used in the calibration against observed patterns in the fossil record. This out-of-sample validation provides a rigorous test of the model ability to capture the macroevolutionary dynamics of real ecosystems.

4.3.3 Exploration of the Phase Space

Once calibrated, the model is used to explore the parameter space defined by the three order parameters of the unified framework: system resilience, environmental pressure, and evolutionary potential. By systematically varying these parameters across thousands of simulation runs, I map the phase diagram of the model, identifying the regions of parameter space that correspond to stable high-diversity states, mass extinctions, and evolutionary radiations (Appendix).

This phase diagram provides a quantitative representation of the unified critical transition model, mapping the conditions under which the ecosystem crosses critical thresholds. The phase diagram can be compared directly with empirical data from specific geological intervals, testing whether the observed patterns of diversity change are consistent with the model predictions.

4.4 Empirical Case Studies: Testing the Unified Framework

I identify four geological intervals that provide critical tests of the unified framework: the Ediacaran-Cambrian transition, the Permian-Triassic transition, the Triassic-Jurassic transition, and the Cretaceous-Paleogene transition. Each interval represents a different configuration of the three order parameters, allowing the model to be tested across a range of conditions (Appendix).

4.4.1 The Cambrian Explosion as an Innovation-Led Radiation

The Cambrian explosion represents a case in which evolutionary potential was high due to the prior evolution of developmental toolkits, including the Hox gene complex, and environmental conditions were permissive due to rising oxygen levels and nutrient availability. The ecosystem transitioned from a low-diversity, low-connectivity state to a high-diversity, high-connectivity state as the establishment of predator-prey interactions created a percolating network structure.

The model predicts that the Cambrian radiation should be characterized by a rapid increase in network connectance and modularity, driven by the evolution of macrophagy and the establishment of multi-trophic food webs. The ecological opportunity created by the decline of the Ediacaran biota provided the initial niche space, while key innovations in sensory systems, locomotion, and skeletonization enabled the rapid filling of that space.

4.4.2 The End-Permian Extinction as a Resilience-Limited Collapse

The end-Permian mass extinction represents a case in which extreme environmental pressure, driven by Siberian Traps volcanism, overwhelmed a system whose resilience may have already been compromised by pre-existing environmental conditions. The late Permian was characterized by a hothouse climate with sluggish oceanic circulation that was leading to widespread oceanic anoxia (Saunders and Reichow, 2009). The combination of low baseline resilience and intense environmental perturbation triggered a catastrophic collapse of the high-diversity state.

The model predicts that the Permian-Triassic interval should exhibit clear early warning signals of critical slowing down in the period preceding the main extinction pulse. The collapse of network connectivity should be evident in the fossil record as the selective extinction of highly connected species triggers secondary extinctions throughout the food web.

4.4.3 The Triassic-Jurassic Extinction and Subsequent Radiation

The end-Triassic mass extinction, triggered by Central Atlantic Magmatic Province volcanism, eliminated approximately 50% of marine genera and created the ecological opportunity for the subsequent Jurassic radiation (Whiteside et al., 2010). This interval provides a test of the model predictions regarding the relationship between extinction magnitude and recovery dynamics.

The model predicts that the recovery from the end-Triassic extinction should be influenced by the evolutionary potential of surviving lineages, the resilience of the post-extinction ecosystem, and the trajectory of environmental recovery. The timing and magnitude of the Jurassic radiation should be predictable from the model phase diagram given the parameter values estimated for this interval.

4.4.4 The K-Pg Mass Extinction and Mammalian Radiation

The end-Cretaceous mass extinction, driven primarily by the Chicxulub impact, eliminated the non-avian dinosaurs and created the ecological opportunity for the Cenozoic radiation of mammals. This interval is particularly informative because it illustrates the role of ecological opportunity in triggering radiation: mammals had existed throughout the Mesozoic but remained constrained to small body sizes and limited ecological roles until the extinction of dinosaurs opened niche space.

The model predicts that the magnitude and tempo of the mammalian radiation should be a function of the evolutionary potential of mammals at the time of the extinction, the amount of niche space cleared by the extinction, and the rate of environmental recovery following the impact winter. The comparison of model predictions with the empirical pattern of mammalian diversification provides a test of the unified framework.

5 Conclusions: The Unified Dynamics of Radiations and Extinctions

5.1 The Core Dynamical Insight

The central conclusion of this paper is that evolutionary radiations and mass extinctions are not fundamentally different classes of phenomena but are two manifestations of the same underlying dynamical process: the crossing of critical thresholds in a complex adaptive system. The three order parameters identified by our framework—system resilience, environmental pressure, and evolutionary potential—jointly determine whether the ecosystem is in a stable high-diversity state, whether it is approaching a collapse threshold, or whether it is poised for an explosive radiation.

Mass extinctions occur when environmental pressure exceeds the capacity of the ecosystem to absorb perturbation, a capacity that is determined by the structural properties of the ecological network, including its modularity, functional redundancy, and degree distribution. The same environmental perturbation that triggers a mass extinction in a fragile, low-redundancy ecosystem may produce only minor turnover in a robust, high-redundancy ecosystem. This explains the observed variability in extinction magnitude across different events and different clades.

Evolutionary radiations occur when evolutionary potential exceeds a threshold that depends on the availability of ecological opportunity and the permissiveness of environmental conditions. The evolution of key innovations, such as developmental toolkits, sensory systems, or metabolic pathways, increases evolutionary potential by opening new regions of niche space. The clearing of niche space by mass extinction creates the ecological opportunity for radiation, but radiation does not occur automatically; it requires both the evolutionary capacity to generate new adaptations and environmental conditions that permit those adaptations to establish and spread.

5.2 Implications for Understanding the Cambrian Explosion

The unified framework resolves several long-standing puzzles about the Cambrian explosion. The question of why the bilaterian radiation occurred when it did, despite evidence that the genetic and developmental machinery for building complex animals existed much earlier, is addressed by the distinction between evolutionary potential and the conditions for crossing the innovation threshold. The evolution of Hox genes and other developmental toolkits increased evolutionary potential, but the Cambrian radiation required the coincidence of this potential with permissive environmental conditions, including sufficient oxygen to support large, active animals, and with the ecological opportunity created by the decline of the Ediacaran biota.

The synchronicity of the radiation across diverse clades is explained by the network percolation dynamics. Once a critical threshold of ecological interactions was established, the evolution of predatory and defensive adaptations created positive feedback loops that accelerated diversification across the entire ecosystem. The establishment of a percolating network of ecological interactions created the structural basis for the stable, high-diversity ecosystem that has characterized the Phanerozoic.

5.3 Implications for Understanding Mass Extinction Variability

The unified framework addresses the question of why mass extinctions vary so dramatically in magnitude and selectivity. The end-Permian mass extinction, the most severe in Earth history, occurred when extreme environmental pressure from the Siberian Traps coincided with a pre-existing state of low resilience in the late Permian ecosystem, characterized by widespread marine anoxia and a hothouse climate (Saunders and Reichow, 2009; Wignall and Twitchett, 1996). The end-Cretaceous mass extinction, while severe, was less catastrophic because the pre-extinction ecosystem, although subject to Deccan Traps volcanism, retained significant resilience, and the post-impact recovery was relatively rapid due to the availability of ecological opportunity and the evolutionary potential of surviving lineages.

The selectivity of extinction—the pattern of which clades survive and which perish—is explained by the relationship between network position and extinction risk. Species occupying hub positions in ecological networks, upon which many other species depend, are more vulnerable to cascade-driven extinction than species in peripheral positions. Functional groups with high redundancy are more likely to survive than groups with low redundancy, because the loss of some species can be compensated by others. This network perspective on extinction selectivity complements the traditional focus on organismal traits such as body size, geographic range, and physiological tolerance.

5.4 Implications for Contemporary Biodiversity Loss

The unified framework carries sobering implications for the contemporary biodiversity crisis. Human activities are simultaneously reducing system resilience by eliminating functional redundancy through species extinctions and habitat fragmentation, increasing environmental pressure through climate change, pollution, and land-use change, and potentially constraining evolutionary potential by reducing population sizes and genetic diversity (Barnosky et al., 2011; Ceballos et al., 2015).

The model predicts that when system resilience falls below a critical threshold, even moderate additional environmental pressure may trigger a catastrophic transition to a low-diversity state. The detection of early warning signals in contemporary ecological data—increasing variance and autocorrelation in population time series, slowing recovery from perturbations—would indicate that ecosystems are approaching critical thresholds and that a transition to an alternative, less diverse state may be imminent.

The lessons from the geological past are clear but not deterministic. Mass extinctions in the Phanerozoic were followed by recoveries, but these recoveries took millions of years and resulted in ecosystems structurally different from those that preceded them (Chen and Benton, 2012). The evolutionary potential for recovery exists, but the timescale of recovery is so far beyond human planning horizons as to be essentially irrelevant for contemporary conservation. The most prudent course, from the perspective of the unified framework, is to maintain system resilience by preserving functional diversity and ecological connectivity while reducing environmental pressure to levels that do not threaten critical thresholds.

5.5 Testable Predictions

The unified framework generates several testable predictions that distinguish it from alternative models.

(1) The model predicts that ecological network structure should exhibit systematic changes in the intervals preceding mass extinctions, including decreasing modularity and increasing vulnerability to cascade-driven collapse. These changes should be detectable through analysis of fossil co-occurrence patterns and functional trait distributions.

(2) The model predicts that early warning signals of critical slowing down—increasing autocorrelation and variance in diversity time series—should be detectable in the intervals immediately preceding major extinction events. The absence of such signals would represent evidence against the critical transition model.

(3) The model predicts that the magnitude of extinction should be correlated with pre-extinction measures of system fragility, including low functional redundancy and high network connectance. This prediction can be tested by comparing extinction magnitudes across different events and different regions with estimates of pre-extinction ecosystem properties.

(4) The model predicts that the tempo of recovery following mass extinctions should be correlated with the evolutionary potential of surviving lineages and the rate of environmental amelioration. This prediction can be tested by comparing recovery dynamics across different extinction events and different clades.

6 Discussion and Perspective

6.1 Limitations of the Current Framework

The unified critical transition model, while providing a coherent framework for understanding macroevolutionary dynamics, has significant limitations that must be acknowledged. The model operates at a high level of abstraction, characterizing the global ecosystem in terms of a small number of macroscopic order parameters. This abstraction inevitably neglects the rich detail of specific evolutionary and ecological processes that operate at finer scales.

The model treats evolutionary innovations as an exogenous input, characterized by the parameter I, rather than as an endogenous product of the evolutionary dynamics themselves. A more complete model would

incorporate feedback between ecological dynamics and the generation of evolutionary novelty, capturing the ways in which ecological opportunity stimulates innovation and innovation creates new ecological opportunity.

The application of the model to empirical data is constrained by the incompleteness of the fossil record and the challenges of reconstructing ecological networks from paleontological data. The spatial and temporal resolution of the fossil record may be insufficient to capture the detailed dynamics near critical thresholds, and preservation biases may distort the patterns that the model predicts.

The model assumes that the global ecosystem can be characterized by a single set of order parameters, but real ecosystems are spatially heterogeneous, with different regions experiencing different environmental conditions and harboring different ecological communities. The extension of the framework to spatially explicit settings, in which different regions may be at different positions relative to critical thresholds, represents an important direction for future work.

6.2 Relationship to Adjacent Theoretical Frameworks

The unified framework presented here engages with several adjacent theoretical traditions that merit explicit discussion.

The framework extends the theory of adaptive radiations, which has emphasized the role of ecological opportunity and key innovations in driving diversification (Simpson, 1953; Schluter, 2000; Losos, 2010), by embedding these concepts within a dynamical systems framework that specifies the conditions under which ecological opportunity translates into explosive radiation versus gradual diversification.

The framework engages with the metabolic theory of ecology (Brown et al., 2004) by providing a complementary perspective on the constraints that govern macroevolutionary dynamics. While metabolic theory emphasizes the energetic constraints on individual organisms and populations, the critical transition framework emphasizes the systemic constraints that arise from the structure of ecological networks and the dynamics of the adaptive landscape.

The framework also engages with evolutionary developmental biology (Carroll, 2006; Erwin and Davidson, 2002) by incorporating developmental innovations as key drivers of evolutionary potential. The formalization of evolutionary potential as an order parameter in the dynamical model provides a bridge between the mechanistic insights of developmental biology and the macroscopic patterns of macroevolution.

6.3 Future Directions

Several directions for future research emerge from this framework.

The most pressing priority is the empirical testing of the model predictions using paleontological data. The application of the early warning signal detection methodology to high-resolution stratigraphic sections spanning major extinction boundaries will provide direct tests of the critical transition model. The reconstruction of paleoecological networks using the computational methods described in Section 4 will enable the testing of predictions regarding network structure and extinction vulnerability.

The extension of the model to spatially explicit settings, in which the global ecosystem is represented as a network of coupled regional ecosystems, represents an important theoretical development. Such an extension would enable the investigation of spatial cascades, in which the collapse of one region triggers collapse in adjacent regions, and spatial refugia, in which some regions escape extinction while others are devastated.

The integration of genomic and phylogenetic data with the fossil record represents another important direction. Molecular phylogenies provide information about the timing and tempo of diversification that complements the fossil record, and genomic data provide information about the genetic basis of evolutionary innovations that drive radiations. The integration of these data sources into a unified analytical framework has the potential to significantly refine our understanding of macroevolutionary dynamics.

6.4 Concluding Remarks

The question of why species experience explosive radiations and catastrophic extinctions is one of the most fundamental in evolutionary biology. The unified critical transition framework developed in this paper provides a new way of approaching this question, one that emphasizes the systemic properties of ecosystems rather than the specific triggers of individual events. By treating radiations and extinctions as two manifestations of the same underlying dynamics, i.e., the crossing of critical thresholds in a complex adaptive system, the framework offers a coherent theoretical foundation for understanding the most dramatic events in the history of life.

The practical implications of this framework extend beyond paleontology. The recognition that ecosystem collapse is a threshold phenomenon, with detectable early warning signals, provides a scientific basis for anticipating and potentially averting future biodiversity crises. The geological record offers a cautionary tale: ecosystems can change abruptly and irreversibly when critical thresholds are crossed. The challenge for contemporary society is to care for that warning.

References

Albert R, Jeong H, Barabási AL. 2000. Error and attack tolerance of complex networks. Nature, 406: 378-382. https://www.nature.com/articles/35019019

Algeo TJ, Shen J. 2024. Theory and classification of mass extinction causation. National Science Review, 11(1): nwad237. https://academic.oup.com/nsr/article/11/1/nwad237/7264266

Allesina S, Tang S. 2012. Stability criteria for complex ecosystems. Nature, 483: 205-208. https://www.nature.com/articles/nature10832

Alroy J. 2010. Fair sampling of taxonomic richness and unbiased estimation of origination and extinction rates. The Paleontological Society Papers, 16: 55-80. https://www.cambridge.org/core/journals/the-paleontological-society-papers/article/abs/fair-sampling-of-taxonomic-richness-and-unbiased-estimation-of-origination-and-extinction-rates/F4E5329EB9A76CC317A591E2A3FA41D4

Alvarez LW, Alvarez W, Asaro F, Michel HV. 1980. Extraterrestrial cause for the Cretaceous-Tertiary extinction. Science, 208(4448): 1095-1108. https://www.science.org/doi/10.1126/science.208.4448.1095

Arnold SJ, Pfrender ME, Jones AG. 2001. The adaptive landscape as a conceptual bridge between micro- and macroevolution. Genetica, 112: 9-32. https://link.springer.com/article/10.1023/A:1013373907708

Bailer-Jones CAL. 2009. The evidence for and against astronomical impacts on climate change and mass extinctions: A review. International Journal of Astrobiology, 8(3): 213-219. https://www.cambridge.org/core/journals/international-journal-of-astrobiology/article/evidence-for-and-against-astronomical-impacts-on-climate-change-and-mass-extinctions-a-review/734B16177C6E03B0D8BA6B2842F217AC

Bak P, Sneppen K. 1993. Punctuated equilibrium and criticality in a simple model of evolution. Physical Review Letters, 71: 4083-4086. https://journals.aps.org/prl/abstract/10.1103/PhysRevLett.71.4083

Barnosky AD. 2001. Distinguishing the effects of the Red Queen and Court Jester on Miocene mammal evolution in the northern Rocky Mountains. Journal of Vertebrate Paleontology, 21(1): 172-185. https://www.tandfonline.com/doi/abs/10.1671/0272-4634(2001)021[0172:DTEOTR]2.0.CO;2

Barnosky AD, Matzke N, Tomiya S, Wogan GOU, Swartz B, Quental TB, et al. 2011. Has the Earth sixth mass extinction already arrived? Nature, 471: 51-57. https://www.nature.com/articles/nature09678

Benton MJ. 2003. When Life Nearly Died: The Greatest Mass Extinction of All Time. Thames and Hudson, London, UK. https://www.thamesandhudson.com/when-life-nearly-died-9780500291931

Benton MJ. 2009. The Red Queen and the Court Jester: Species diversity and the role of biotic and abiotic factors through time. Science, 323(5915): 728-732. https://www.science.org/doi/10.1126/science.1157719

Black BA, Elkins-Tanton LT, Rowe MC, Peate IU. 2012. Magnitude and consequences of volatile release from the Siberian Traps. Earth and Planetary Science Letters, 317-318: 363-373. https://www.sciencedirect.com/science/article/pii/S0012821X11007151

Bond DPG, Grasby SE. 2017. On the causes of mass extinctions. Palaeogeography, Palaeoclimatology, Palaeoecology, 478: 3-29. https://www.sciencedirect.com/science/article/pii/S0031018216306915

Bond DPG, Wignall PB. 2008. The role of sea-level change and marine anoxia in the Frasnian-Famennian (Late Devonian) mass extinction. Palaeogeography, Palaeoclimatology, Palaeoecology, 263(3-4): 107-118. https://www.sciencedirect.com/science/article/pii/S0031018208001697

Brasier MD, Lindsay JF. 2001. Did supercontinental amalgamation trigger the Cambrian explosion? In: The Ecology of the Cambrian Radiation (Zhuravlev AY, Riding R,eds). 69-89, Columbia University Press, New York, USA. https://cup.columbia.edu/book/the-ecology-of-the-cambrian-radiation/9780231106139/

Brenchley PJ, Marshall JD, Underwood CJ. 2001. Do all mass extinctions represent an ecological crisis? Evidence from the Late Ordovician. Geological Journal, 36: 329-340. https://onlinelibrary.wiley.com/doi/abs/10.1002/gj.880

Brennan ST, Lowenstein TK, Horita J. 2004. Seawater chemistry and the advent of biocalcification. Geology, 32(6): 473-476. https://pubs.geoscienceworld.org/gsa/geology/article/32/6/473/29431/Seawater-chemistry-and-the-advent-of?guestAccessKey=

Brown JH, Gillooly JF, Allen AP, Savage VM, West GB. 2004. Toward a metabolic theory of ecology. Ecology, 85(7): 1771-1789. https://esajournals.onlinelibrary.wiley.com/doi/10.1890/03-9000

Burgess SD, Bowring SA, Shen SZ. 2014. High-precision timeline for Earth most severe extinction. Proceedings of the National Academy of Sciences, 111(9): 3316-3321. https://www.pnas.org/doi/10.1073/pnas.1317692111

Canfield DE, Poulton SW, Narbonne GM. 2007. Late-Neoproterozoic deep-ocean oxygenation and the rise of animal life. Science, 315(5808): 92-95. https://www.science.org/doi/10.1126/science.1135013

Carroll SB. 2006. Endless Forms Most Beautiful: The New Science of Evo Devo. W.W. Norton, New York, USA. https://wwnorton.com/books/Endless-Forms-Most-Beautiful/

Ceballos G, Ehrlich PR, Barnosky AD, García A, et al. 2015. Accelerated modern human-induced species losses: Entering the sixth mass extinction. Science Advances, 1(5): e1400253. https://www.science.org/doi/10.1126/sciadv.1400253

Chen ZQ, Benton MJ. 2012. The timing and pattern of biotic recovery following the end-Permian mass extinction. Nature Geoscience, 5: 375-383. https://www.nature.com/articles/ngeo1475

Dakos V, Scheffer M, van Nes EH, et al. 2008. Slowing down as an early warning signal for abrupt climate change. Proceedings of the National Academy of Sciences of USA, 105(38): 14308-14312. https://www.pnas.org/doi/10.1073/pnas.0802430105

Darroch SAF, Sperling EA, Boag TH, et al. 2015. Biotic replacement and mass extinction of the Ediacara biota. Proceedings of the Royal Society B, 282(1814): 20151003. https://royalsocietypublishing.org/rspb/article/282/1814/20151003/84270/Biotic-replacement-and-mass-extinction-of-the

Davies JHFL, Marzoli A, Bertrand H, Youbi N, et al. 2017. End-Triassic mass extinction started by intrusive CAMP activity. Nature Communications, 8: 15596. https://www.nature.com/articles/ncomms15596

Douzery EJP, Snell EA, Bapteste E, et al. 2004. The timing of eukaryotic evolution: Does a relaxed molecular clock reconcile proteins and fossils? Proceedings of the National Academy of Sciences of USA, 101(43): 15386-15391. https://www.pnas.org/doi/10.1073/pnas.0403984101

Du MH, Wang WH, Tan JQ, et al. 2024. Deep learning for mass extinction detection on fossilized phylogenies: Power, limitations, and lessons for simulation-based phylodynamic inference. bioRxiv. https://www.biorxiv.org/content/10.1101/2025.10.20.683352v1.full.pdf

Dunne JA, Williams RJ. 2009. Cascading extinctions and community collapse in model food webs. Philosophical Transactions of the Royal Society B, 364(1524): 1711-1723. https://royalsocietypublishing.org/rstb/article/364/1524/1711/57853/Cascading-extinctions-and-community-collapse-in

Dunne JA, Williams RJ, Martinez ND, Wood RA, Erwin DH. 2008. Compilation and network analyses of Cambrian food webs. PLoS Biology, 6: e102. https://journals.plos.org/plosbiology/article?id=10.1371/journal.pbio.0060102

Eldredge N, Gould SJ. 1972. Punctuated equilibria: An alternative to phyletic gradualism. In: Models in Paleobiology (Schopf TJM, ed). 82-115, Freeman Cooper, San Francisco, USA. https://philpapers.org/rec/ELDOPE

Erwin DH. 1998. The end and the beginning: Recoveries from mass extinctions. Trends in Ecology and Evolution, 13(9): 344-349. https://www.sciencedirect.com/science/article/pii/S0169534798014360

Erwin DH. 2006. Extinction: How Life on Earth Nearly Ended 250 Million Years Ago. Princeton University Press, Princeton, USA. https://press.princeton.edu/books/paperback/9780691165653/extinction

Erwin DH, Davidson EH. 2002. The last common bilaterian ancestor. Development, 129(13): 3021-3032. https://journals.biologists.com/dev/article/129/13/3021/41745/The-last-common-bilaterian-ancestor

Erwin DH, Laflamme M, Tweedt SM, Sperling EA, et al. 2011. The Cambrian conundrum: Early divergence and later ecological success in the early history of animals. Science, 334(6059): 1091-1097. https://www.science.org/doi/10.1126/science.1206375

Erwin DH, Valentine JW. 2013. The Cambrian Explosion: The Construction of Animal Biodiversity. Roberts and Company, Greenwood Village, USA. https://www.journals.uchicago.edu/doi/10.1086/681449

Finnegan S, Bergmann K, Eiler JM, et al. 2011. The magnitude and duration of Late Ordovician-Early Silurian glaciation. Science, 331(6019): 903-906. https://www.science.org/doi/10.1126/science.1200803

Folke C, Carpenter S, Walker B, Scheffer M, Elmqvist T, Gunderson L, Holling CS. 2004. Regime shifts, resilience, and biodiversity in ecosystem management. Annual Review of Ecology, Evolution, and Systematics, 35: 557-581. https://www.annualreviews.org/content/journals/10.1146/annurev.ecolsys.35.021103.105711

Gould SJ, Eldredge N. 1977. Punctuated equilibria: The tempo and mode of evolution reconsidered. Paleobiology, 3(2): 115-151. https://www.cambridge.org/core/journals/paleobiology/article/abs/punctuated-equilibria-the-tempo-and-mode-of-evolution-reconsidered/416469B94B074D3F7311C805274679D4

Grant PR, Grant BR. 2011. How and Why Species Multiply: The Radiation of Darwin Finches. Princeton University Press, Princeton, USA. https://press.princeton.edu/books/paperback/9780691149998/how-and-why-species-multiply

Grasby SE, Them II TR, Chen ZH, Yin RS, Ardakani OH. 2019. Mercury as a proxy for volcanic emissions in the geologic record. Earth-Science Reviews, 196: 102880. https://www.sciencedirect.com/science/article/pii/S0012825219301588

Grice K, Cao CQ, Love GD, Böttcher ME, et al. 2005. Photic zone euxinia during the Permian-Triassic superanoxic event. Science, 307(5710): 706-709. https://www.science.org/doi/10.1126/science.1104323

Harper DAT, Hammarlund EU, Rasmussen CMØ. 2014. End Ordovician extinctions: A coincidence of causes. Gondwana Research, 25(4): 1294-1307. https://www.sciencedirect.com/science/article/pii/S1342937X13000154

Hautmann M, Benton MJ, Tomašových A. 2008. Catastrophic ocean acidification at the Triassic-Jurassic boundary. Neues Jahrbuch für Geologie und Paläontologie, 249(1): 119-127. https://bpb-eu-w2.wpmucdn.com/blogs.bristol.ac.uk/dist/5/537/files/2019/07/2008Hautmann.pdf

Holling CS. 1973. Resilience and stability of ecological systems. Annual Review of Ecology and Systematics, 4: 1-23. https://www.annualreviews.org/content/journals/10.1146/annurev.es.04.110173.000245

Jablonski D. 2008. Extinction and the spatial dynamics of biodiversity. Proceedings of the National Academy of Sciences of USA, 105(Suppl): 11528-11535. https://www.pnas.org/doi/10.1073/pnas.0801919105

Kärenlampi PP. 2015. Extremal dynamics in random replicator ecosystems. Physica A, 379(37): 2209-2214. https://www.sciencedirect.com/science/article/pii/S0375960115006301?via%3Dihub

Keller G. 2014. Deccan volcanism, the Chicxulub impact, and the end-Cretaceous mass extinction: coincidence? Cause and effect? Geological Society of America Special Papers, 505: 57-89. https://onlinelibrary.wiley.com/doi/10.1111/j.1365-2486.2010.02204.x

Kiessling W, Simpson C. 2011. On the potential for ocean acidification to be a general cause of ancient reef crises. Global Change Biology, 17: 56-67. https://onlinelibrary.wiley.com/doi/10.1111/j.1365-2486.2010.02204.x

Knauth LP. 2005. Temperature and salinity history of the Precambrian ocean: Implications for the course of microbial evolution. Palaeogeography, Palaeoclimatology, Palaeoecology, 219(1-2): 53-69. https://www.sciencedirect.com/science/article/pii/S0031018204005905

Knoll AH, Carroll SB. 1999. Early animal evolution: Emerging views from comparative biology and geology. Science, 284(5423): 2129-2137. https://www.science.org/doi/10.1126/science.284.5423.2129

Kondoh M. 2003. Foraging adaptation and the relationship between food-web complexity and stability. Science, 299(5611): 1388-1391. https://www.science.org/doi/10.1126/science.1079154

Kramers HA. 1940. Brownian motion in a field of force and the diffusion model of chemical reactions. Physica, 7(4): 284-304. https://www.sciencedirect.com/science/article/abs/pii/S0031891440900982

Li MG, Grasby SE, Wang SJ, Zhang XL, et al. 2021. Nickel isotopes link Siberian Traps aerosol particles to the end-Permian mass extinction. Nature Communications, 12: 2024. https://www.nature.com/articles/s41467-021-22066-7

Losos JB. 2010. Adaptive radiation, ecological opportunity, and evolutionary determinism. The American Naturalist, 175(6): 623-639. https://www.journals.uchicago.edu/doi/10.1086/652433

Losos JB. 2011. Lizards in an Evolutionary Tree: Ecology and Adaptive Radiation of Anoles. University of California Press, Berkeley, USA. https://www.ucpress.edu/book/9780520269842/lizards-in-an-evolutionary-tree

Lyons TW, Reinhard CT, Planavsky NJ. 2014. The rise of oxygen in Earth early ocean and atmosphere. Nature, 506: 307-315. https://www.nature.com/articles/nature13068

Marshall CR. 2006. Explaining the Cambrian explosion of animals. Annual Review of Earth and Planetary Sciences, 34: 355-384. https://www.annualreviews.org/content/journals/10.1146/annurev.earth.33.031504.103001

May RM. 1972. Will a large complex system be stable? Nature, 238: 413-414. https://www.nature.com/articles/238413a0

Mills DB, Ward LM, Jones CA, et al. 2014. Oxygen requirements of the earliest animals. Proceedings of the National Academy of Sciences, 111(11): 4168-4172. https://www.pnas.org/doi/10.1073/pnas.1400547111

Molloy M, Reed B. 1995. A critical point for random graphs with a given degree sequence. Random Structures and Algorithms, 6: 161-180. https://onlinelibrary.wiley.com/doi/10.1002/rsa.3240060204

Morgan JV, Bralower TJ, Brugger J, Wünnemann K. 2022. The Chicxulub impact and its environmental consequences. Nature Reviews Earth and Environment, 3: 338-354. https://www.nature.com/articles/s43017-022-00283-y

Newman MEJ. 1997. A model of mass extinction. Journal of Theoretical Biology, 189: 235-252. https://www.sciencedirect.com/science/article/abs/pii/S002251939790510X

Newman MEJ. 2006. Modularity and community structure in networks. Proceedings of the National Academy of Sciences of USA, 103(23): 8577-8582. https://www.pnas.org/doi/10.1073/pnas.0601602103

Newman MEJ, Palmer RG. 2003. Modeling Extinction. Oxford University Press, Oxford, UK. https://global.oup.com/academic/product/modeling-extinction-9780195159462?cc=sg&lang=en&

Ohno S, Kadono T, Kurosawa K, Hamura T, et al. 2014. Production of sulphate-rich vapour during the Chicxulub impact and implications for ocean acidification. Nature Geoscience, 7: 279-282. https://www.nature.com/articles/ngeo2095

Peters SE, Gaines RR. 2012. Formation of the Great Unconformity as a trigger for the Cambrian explosion. Nature, 484: 363-366. https://www.nature.com/articles/nature10969

Rabosky DL, Hurlbert AH. 2015. Species richness at continental scales is dominated by ecological limits. The American Naturalist, 185(5): 572-583. https://www.journals.uchicago.edu/doi/10.1086/680850

Raup DM, Sepkoski JR JJ. 1982. Mass extinctions in the marine fossil record. Science, 215(4539): 1501-1503. https://www.science.org/doi/10.1126/science.215.4539.1501

Reddy S, Driskell A, Rabosky DL, Hackett SJ, Schulenberg TS. 2012. Diversification and the adaptive radiation of the vangas of Madagascar. Proceedings of the Royal Society B, 279: 2062-2071. https://royalsocietypublishing.org/rspb/article/279/1735/2062/74089/Diversification-and-the-adaptive-radiation-of-the

Robertson DS, Lewis WM, Sheehan PM, Toon OB. 2013. K-Pg extinction: Reevaluation of the heat-fire hypothesis. Journal of Geophysical Research: Biogeosciences, 118: 329-336. https://agupubs.onlinelibrary.wiley.com/doi/10.1002/jgrg.20018

Saunders AD, Reichow MK. 2009. The Siberian Traps and the End-Permian mass extinction: A critical review. Chinese Science Bulletin, 54: 20-37. https://link.springer.com/article/10.1007/s11434-008-0543-7

Scheffer M. 2009. Critical Transitions in Nature and Society. Princeton University Press, Princeton, USA. https://press.princeton.edu/books/paperback/9780691122045/critical-transitions-in-nature-and-society

Scheffer M, Bascompte J, Brock WA, Brovkin V, et al. 2009. Early-warning signals for critical transitions. Nature, 461: 53-59. https://www.nature.com/articles/nature08227

Scheffer M, Carpenter S, Foley JA, Folke C, Walker B. 2001. Catastrophic shifts in ecosystems. Nature, 413: 591-596. https://www.nature.com/articles/35098000

Scheffer M, Carpenter SR, Lenton TM, Bascompte J, et al. 2012. Anticipating critical transitions. Science, 338(6105): 344-348. https://www.science.org/doi/10.1126/science.1225244

Schluter D. 2000. The Ecology of Adaptive Radiation. Oxford University Press, Oxford, UK. https://global.oup.com/academic/product/the-ecology-of-adaptive-radiation-9780198505228?cc=sg&lang=en&

Schoene B, Eddy MP, Samperton KM, Keller CB, et al. 2019. U-Pb constraints on pulsed eruption of the Deccan Traps across the end-Cretaceous mass extinction. Science, 363(6429): 862-866. https://www.science.org/doi/10.1126/science.aau2422

Schulte P, Alegret L, Arenillas I, Arz JA, et al. 2010. The Chicxulub asteroid impact and mass extinction at the Cretaceous-Paleogene boundary. Science, 327(5970): 1214-1218. https://www.science.org/doi/10.1126/science.1177265

Shams B, Khansari M. 2014. Using network properties to evaluate targeted immunization algorithms. Network Biology, 4(3): 74-94. http://www.iaees.org/publications/journals/nb/articles/2014-4(3)/1-Khansari-Abstract.asp

Shen SZ, Zhang H. 2017. What caused the biological mass extinctions? Chinese Science Bulletin, 62(11): 1119-1135. https://www.sciengine.com/CSB/doi/10.1360/N972017-00013

Simpson GG. 1984. Tempo and Mode in Evolution. Columbia University Press, New York, USA. https://cup.columbia.edu/book/tempo-and-mode-in-evolution/9780231058476/

Simpson GG. 1953. The Major Features of Evolution. Columbia University Press, New York, USA. https://www.amazon.com/Major-Features-Evolution-G-SIMPSON/dp/0231018215

Smart MS, Filippelli G, Gilhooly III WP, et al. 2023. The expansion of land plants during the Late Devonian contributed to the marine mass extinction. Communications Earth and Environment, 4: 449. https://www.nature.com/articles/s43247-023-01087-8

Sneppen K, Bak P, Flyvbjerg H, Jensen MH. 1995. Evolution as a self-organized critical phenomenon. Proceedings of the National Academy of Sciences, 92(11): 5209-5213. https://www.pnas.org/doi/10.1073/pnas.92.11.5209

Sperling EA, Frieder CA, Raman AV, et al. 2013. Oxygen, ecology, and the Cambrian radiation of animals. Proceedings of the National Academy of Sciences, 110(3): 13446-13451. https://www.pnas.org/doi/10.1073/pnas.1312778110

Svensen H, Planke S, Polozov AG, Schmidbauer N, Corfu F, Podladchikov YY, Jamtveit B. 2009. Siberian gas venting and the end-Permian environmental crisis. Earth and Planetary Science Letters, 277(3-4): 490-500. https://www.sciencedirect.com/science/article/pii/S0012821X08007292

Valentine JW. 2006. On the Origin of Phyla. University of Chicago Press, Chicago, USA. https://press.uchicago.edu/ucp/books/book/chicago/O/bo3616676.html

Van Valen L. 1973. A new evolutionary law. Evolutionary Theory, 1: 1-30. https://www.mn.uio.no/cees/english/services/van-valen/evolutionary-theory/volume-1/vol-1-no-1-pages-1-30-l-van-valen-a-new-evolutionary-law.pdf

Vellekoop J, Sluijs A, Smit J, et al. 2014. Rapid short-term cooling following the Chicxulub impact at the Cretaceous-Paleogene boundary. Proceedings of the National Academy of Sciences of USA, 111(21): 7537-7541. https://www.pnas.org/doi/10.1073/pnas.1319253111

Whiteside JH, Olsen PE, Eglington T, et al. 2010. Compound-specific carbon isotopes from Earth largest flood basalt eruptions directly linked to the end-Triassic mass extinction. Proceedings of the National Academy of Sciences of USA, 107(15): 6721-6725. https://www.pnas.org/doi/10.1073/pnas.1001706107

Wignall PB. 2015. The Worst of Times: How Life on Earth Survived Eighty Million Years of Extinctions. Princeton University Press, Princeton, USA. https://press.princeton.edu/books/hardcover/9780691142098/the-worst-of-times

Wignall PB, Twitchett RJ. 1996. Oceanic anoxia and the end Permian mass extinction. Science, 272(5265): 1155-1158. https://www.science.org/doi/10.1126/science.272.5265.1155

Wright S. 1932. The roles of mutation, inbreeding, crossbreeding and selection in evolution. Proceedings of the Sixth International Congress of Genetics, 1: 356-366. https://www.blackwellpublishing.com/ridley/classictexts/wright.pdf

Wu SH, Zhang WJ. 2012. Current status, crisis and conservation of coral reef ecosystems in China. Proceedings of the International Academy of Ecology and Environmental Sciences, 2(1): 1-11. http://www.iaees.org/publications/journals/piaees/articles/2012-2(1)/current-status-crisis-and-conservation-of-coral-reef-ecosystems.pdf

Xin SH, Zhang WJ. 2020. Construction and analysis of the protein-protein interaction network for the olfactory system of the silkworm Bombyx mori. Archives of Insect Biochemistry and Physiology, 105(3): e21737. https://onlinelibrary.wiley.com/doi/10.1002/arch.21737

Zhang WJ. 2011. Constructing ecological interaction networks by correlation analysis: Hints from community sampling. Network Biology, 1(2): 81-98. http://www.iaees.org/publications/journals/nb/articles/2011-1(2)/Constructing-ecological-interaction-networks-by-correlation-analysis.pdf

Zhang WJ. 2012a. Computational Ecology: Graphs, Networks and Agent-based Modeling. World Scientific, Singapore. https://www.worldscientific.com/worldscibooks/10.1142/8118#t=aboutBook

Zhang WJ. 2012b. Modeling community succession and assembly: A novel method for network evolution. Network Biology, 2(2): 69-78. http://www.iaees.org/publications/journals/nb/articles/2012-2(2)/modeling-community-succession-and-assembly.pdf

Zhang WJ. 2015. A generalized network evolution model and self-organization theory on community assembly. Selforganizology, 2(3): 55-64. http://www.iaees.org/publications/journals/selforganizology/articles/2015-2(3)/A-network-evolution-model-and-self-organization-theory.pdf

Zhang WJ. 2016a. A method for identifying hierarchical sub-networks / modules and weighting network links based on their similarity in sub-network / module affiliation. Network Pharmacology, 1(2): 54-65

Zhang WJ. 2016b. Selforganizology: The Science of Self-Organization. World Scientific, Singapore. https://www.worldscientific.com/worldscibooks/10.1142/9685#t=aboutBook

Zhang WJ. 2017. Phase recognition in network evolution. Selforganizology, 4(3): 35-40. http://www.iaees.org/publications/journals/selforganizology/articles/2017-4(3)/phase-recognition-in-network-evolution.pdf

Zhang WJ. 2018. Fundamentals of Network Biology. World Scientific Europe, London, UK. https://www.worldscientific.com/worldscibooks/10.1142/q0149#t=aboutBook

Zhang WJ. 2021. Construction and analysis of the word network based on the Random Reading Frame (RRF) method. Network Biology, 11(3): 154-193. http://www.iaees.org/publications/journals/nb/articles/2021-11(3)/construction-and-analysis-of-word-network-from-Random-Reading-Frame.pdf

Zhang WJ. 2023. netAna: A tool for network analysis. Network Biology, 13(4): 192-212. http://www.iaees.org/publications/journals/nb/articles/2023-13(4)/6-Zhang-Abstract.asp

Zhang WJ. 2026a. Estimating global species richness: A hierarchical weighted cross-calibration approach. Computational Ecology and Software, 16(3): 220-242. http://www.iaees.org/publications/journals/ces/articles/2026-16(3)/2-Zhang-Abstract.asp

Zhang WJ. 2026b. The Niche-Energy-Time triadic synergy hypothesis (NET Hypothesis): A unified explanatory framework for determinants of species diversity. Computational Ecology and Software, 16(3): 243-272. http://www.iaees.org/publications/journals/ces/articles/2026-16(3)/3-Zhang-Abstract.asp

Zhang GL, Zhang WJ. 2019. Protein-protein interaction network analysis of insecticide resistance molecular mechanism in Drosophila melanogaster. Archives of Insect Biochemistry and Physiology, 100(1): e21523. https://onlinelibrary.wiley.com/doi/10.1002/arch.21523

Zhang WJ, Li X. 2016. A cluster method for finding node sets / sub-networks based on between- node similarity in sets of adjacency nodes: with application in finding sub-networks in tumor pathways. Proceedings of the International Academy of Ecology and Environmental Sciences, 6(1): 13-23.

http://www.iaees.org/publications/journals/piaees/articles/2016-6(1)/cluster-method-for-finding-node-sets-and-sub-networks.pdf

Zhang XL, Shu DG, Han J, Zhang ZF, Liu JN, Fu DJ. 2014. Triggers for the Cambrian explosion: Hypotheses and problems. Gondwana Research, 25(3): 896-909. https://www.sciencedirect.com/science/article/pii/S1342937X13001779

Appendix

Computational Methods of the Unified Critical Transition Framework

Here are the detailed computational methods and major procedures for the two components described in the paper: (1) the agent-based eco-evolutionary simulation and construction of the phase diagram, and (2) the identification of four geological intervals and mapping of empirical data onto the theoretical phase diagram.

1 Agent-Based Eco-Evolutionary Simulation and Phase Diagram Construction

1.1 Model Specification

The model is an individual-based eco-evolutionary simulation (Zhang, 2012a, 2018). Each species is defined by a vector of continuous traits and interacts with other species through a dynamically constructed food web.

(1) Species state: The state of species i is given by its population density N_i and a trait vector $t_i \in \mathrm{R}^d$. Traits include body size, trophic level, and environmental tolerance range.

(2) Population dynamics: The model uses a generalized Lotka-Volterra formulation:

$$dN_i/dt = r_i N_i \left(1 - \frac{\sum_j \alpha_{ij} N_j}{K_i(t)}\right)$$

where N_i is the population size of species i, r_i is its intrinsic growth rate, α_{ij} is the interaction coefficient representing the effect of species j on species i (positive values represent competitive or predatory pressure, negative values represent mutualistic benefits; the sign convention can be adapted), and $K_i(t)$ is the time-dependent carrying capacity.

(3) Interaction network: The interaction coefficient α_{ij} is determined by trait similarity. If species j falls within the feeding range of species i based on body size and trophic level, then $\alpha_{ij} > 0$ (prey contributes positively to predator growth) and $\alpha_{ji} < 0$ (predator exerts negative pressure on prey). Competition coefficients are computed from niche overlap using a Gaussian kernel over trait space.

(4) Carrying capacity: $K_i(t)$ is expressed as:

$$K_i(t) = K_0 \exp\left(-\frac{(T(t)-T_{\mathrm{opt},i})^2}{2\sigma_T^2}\right)$$

where $T(t)$ is the environmental temperature trajectory, $T_{\mathrm{opt},i}$ is the optimal temperature for species i, and is the tolerance width.

(5) Evolution: At every Δt_{evo} time step, a speciation event occurs with probability p_{spec}. A randomly chosen species splits into two daughter species; the daughter traits are the parent trait plus small Gaussian noise. New interaction coefficients are computed based on the new trait vector. Speciation probability is diversity-dependent: $p_{\mathrm{spec}} = p_0 / (1 + \gamma D)$, where D is the current number of species.

(6) Extinction (Zhang, 2015): A species is removed when $N_i < N_{ext}$. Environmental perturbations are introduced by modifying $T(t)$ over time.

1.2 Parameter Scanning and Control of Order Parameters

The three order parameters *R*, *S*, *I* are not set directly but are controlled through underlying model parameters. The mapping is as follows:

(1) System resilience *R* is determined by functional redundancy and network modularity. In the model, it is controlled by the initial number of functional groups N_{guild} and the variance of interaction strengths σ_α. High redundancy and low variance correspond to high *R*. Parameter ranges scanned: $N_{guild} \in \{3, 5, 7, 10\}$, $\sigma_\alpha \in [0.1, 0.5]$.

(2) Environmental pressure *S* is controlled by the rate of temperature change dT/dt and the total magnitude of change ΔT. Scanned ranges: $dT/dt \in [0, 2]$°C/10^3yr, $\Delta T \in [2, 15]$ °C.

(3) Evolutionary potential *I* is controlled by the baseline speciation probability p_0 and the mutational trait variance σ_{mut}. Scanned ranges: $p_0 \in [0.001, 0.05]$, $\sigma_{mut} \in [0.01, 0.2]$.

A Latin hypercube sampling design is used to draw 5,000 parameter combinations. Each combination is replicated 5 times (with different random seeds) to account for stochasticity, yielding a total of 25,000 simulation runs.

1.3 Simulation Protocol

Each simulation run proceeds as follows:

(1) Initialization: Generate 50 species with random traits. Compute the initial interaction network. Set T_0. Equilibrate the community for 5,000 generations to reach a stable state.

(2) Environmental perturbation: At generation 6,000, apply a linear temperature change with the given rate dT/dt until the target magnitude ΔT is reached; then hold the temperature constant. The simulation continues until generation 20,000.

(3) Data recording: Every 100 generations, record species richness *D*, number of functional groups *G*, network modularity *Q*, total biomass, and other metrics.

(4) Replicate: Repeat the entire run independently 5 times for each parameter set.

1.4 Classification of Macro-States

After each run, the diversity trajectory is used to classify the outcome into one of three states: Stable High Diversity (SHD), Mass Extinction (ME), or Evolutionary Radiation (ER). The classification algorithm is:

(1) Mass Extinction (ME): If, after perturbation onset and before the end of the simulation, species richness drops by more than 75% and the recovered diversity never exceeds 50% of the pre-perturbation value, the run is classified as ME.

(2) Evolutionary Radiation (ER): If, after perturbation, diversity increases to more than 150% of the pre-perturbation value within 10^4 generations, and the number of functional groups increases by more than 20%, the run is classified as ER.

(3) Stable High Diversity (SHD): If neither ME nor ER criteria are met, and diversity fluctuates within ±20% of the pre-perturbation value, the run is classified as SHD.

For each parameter combination, the final classification is the majority state among the 5 replicates. If no majority exists, the point is labeled as transitional.

1.5 Phase Diagram Construction

To construct the two-dimensional phase diagram:

(1) The environmental pressure axis *S* is defined as the first principal component of dT/dt and ΔT.

(2) The system resilience axis *R* is defined as the first principal component of N_{guild} and $1/\sigma_\alpha$.

(3) Points in this (*S*, *R*) plane are colored according to their majority state (ME, ER, SHD).

(4) Contours of equal evolutionary potential I (first principal component of p_0 and σ_{mut}) are overlaid.

The resulting diagram shows a clear ME region at high S and low R, an ER region at intermediate S, high I, and moderate R, and an SHD region at low S and high R, with sharp boundaries between them.

2 Geological Interval Identification and Empirical Mapping

2.1 Selection Criteria and Data Sources

Four geological intervals are selected: the Ediacaran–Cambrian transition (E–C), the Permian–Triassic transition (P–Tr), the Triassic–Jurassic transition (Tr–J), and the Cretaceous–Paleogene transition (K–Pg). Selection criteria:

(1) Well-documented mass extinction and/or major radiation.

(2) Availability of continuous, high-resolution paleontological and geochemical proxy data.

(3) Feasibility of estimating the three order parameters R, S, I from proxy records.

Data sources include fossil occurrence data from the Paleobiology Database (PBDB), carbon and oxygen isotope compilations, mercury concentration records, and paleotemperature reconstructions from published literature.

2.2 Empirical Estimation of Order Parameters R, S, I

(1) Environmental Pressure S

S is estimated as a weighted sum of the maximum rate of carbon isotope excursion and the maximum rate of temperature change:

(a) Extract $\delta^{13}C$ time series from isotope databases. Compute the first difference within a 500-kyr moving window; take the maximum absolute rate $|\delta^{13}C/\Delta t|$.

(b) Obtain paleotemperature estimates from $\delta^{18}O$ records or climate model outputs; similarly compute the maximum rate of temperature change $|\Delta T/\Delta t|$.

(c) Calculate $S = \beta_C \max |\delta^{13}C/\Delta t| + \beta_T \max |\Delta T/\Delta t|$. The coefficients β_C, β_T are determined by principal component analysis such that they maximize the separation between the four events.

(2) Evolutionary Potential I

I is estimated using two proxies: pre-extinction morphological disparity and the amount of vacated niche space:

(a) Morphological disparity is computed from fossil morphometric data (e.g., shape coordinates) as the mean pairwise Euclidean distance among species within the assemblage.

(b) Vacated niche space is estimated as the number of functional groups present before the extinction minus those present immediately after, normalized by the pre-extinction number.

(c) Combine: $I = \gamma_D \text{Disparity}_{pre} + \gamma_N N_{vacant}$, with coefficients γ_D, γ_N determined by factor analysis so that the resulting I values align with the theoretical definition (higher I) for intervals that were followed by large radiations).

(3) System Resilience R

R is estimated from the structure of the pre-extinction ecological network, reconstructed from fossil data:

(a) Network reconstruction: Build a species co-occurrence matrix from PBDB data for the last stable interval before the event (e.g., the 1 Myr prior). Apply Bayesian network inference to identify significant conditional dependencies among taxa, yielding a partial correlation network. Use deep learning-based functional trait inference (a convolutional neural network trained on modern organisms) to predict feeding modes and trophic relationships from fossil morphology. Integrate these to produce a directed food web.

(b) Functional redundancy: $F = \frac{1}{G}\sum_{g=1}^{G}(n_g - 1)$, where G is the number of functional groups (e.g., primary producer, herbivore, carnivore) and n_g is the number of species in group g.

(c) Network modularity: Compute Q using the Louvain community detection algorithm.

(d) Connectance: The undirected connectance $C = 2L / (N(N-1))$, where L is the number of links and N is the number of species.

(e) Combine into resilience: $R = \alpha_F F + \alpha_M Q - \alpha_C C$. The coefficients α_F, α_M, α_C are calibrated from the simulation experiments by regressing the theoretical R (as defined by model parameters) against the empirical network metrics.

2.3 Classification of Geological Intervals

For each geological interval, the pre-perturbation values of R and I are estimated from the last stable interval, and S is estimated from the perturbation phase. These triplets (R, S, I) are projected onto the simulation-derived phase diagram.

(1) E–C transition: Expected to map into the radiation region (high I, moderate S, moderate R).

(2) P–Tr: Expected to map into the extinction region (extremely high S, low R).

(3) Tr–J: Expected to map into the extinction region but with somewhat lower S and slightly higher R than P–Tr.

(4) K–Pg: Expected to map into the extinction region with a very high but short-lived S (impact pulse) and moderate R, possibly influenced by concurrent Deccan volcanism.

In addition, critical slowing down indicators are computed for each interval to test the model's early-warning prediction:

(1) Construct a diversity time series (e.g., number of genera) across the interval.

(2) Use a moving window of width equal to 1/10 of the interval duration. Within each window, compute the lag-1 autocorrelation AR(1) and the standard deviation.

(3) For the period leading up to the extinction horizon, test for a significant increasing trend in AR(1) and variance using the Kendall tau rank correlation. A significant positive trend ($p < 0.05$) is interpreted as empirical evidence of critical slowing down, consistent with the model's dynamics.

This methodology provides a complete pipeline from simulation-based theory to empirical validation, linking the abstract order parameters to measurable proxy data and enabling a direct test of the unified critical transition framework.